Natural Convection in Layered Porous Media between Coaxial Cylinders

Master of Science Thesis in Applied and Computational Mathematics

Bianca Selheim

Department of Mathematics
University of Bergen

June 1, 2015

Acknowledgements

First and foremost I would like to gratefully thank my supervisor Inga Berre for her excellent help, guidance and supervision on this thesis. I would also like to show gratitude to my co-supervisor Carina Bringedal for her great assistance, valuable feedback and never-ending patience with me when I came to her for help. They have both motivated me throughout this project with their positive and enthusiastic attitude. I am also very grateful for the opportunity to travel as part of my degree, and for Inga Berre and Jan M. Nordbotten who made the trip possible. A special thanks to Professor D. Andrew Rees for providing useful advice concerning the solution approach.

My fellow students deserve a lot of credit for adding humour and valuable company to my days at the University. The study period would not have been the same without them. Thanks to all my friends who helped me take my mind of the thesis outside the office. I especially want to express my appreciation to my best friend Anne-Grethe for her moral support and for always being there.

Finally, I am forever grateful for my wonderful parents and beloved grandmother for always supporting and believing in me. It has meant a lot, and made the whole process easier.

Bianca,
May 2015.

Abstract

In this thesis a mathematical model is developed to describe the onset of natural convection in a two-layer porous medium located between two coaxial cylinders, motivated by natural convection processes in geothermal systems. The cylinders are heated from below and cooled from above. We consider the top and bottom to be impermeable and perfectly heat conducting, while the sidewalls are assumed to be impermeable and insulated. At the interface between the layers, we require continuity in temperature, pressure, vertical flow and heat flow.

We apply linear stability analysis to determine the criterion for onset of natural convection in the bottom layer. An investigation of the effects of permeability contrasts between the two layers on the critical Rayleigh number is performed. We present new results, as our analysis applies to a two-layer medium in cylindrical coordinates. The results are validated by comparison with similar previous studies for a single-layer medium with the same geometry, and for a layered medium within a box geometry. The model has real life applications as it may work as an indicator of the presence of natural convection in the subsurface and since the results can be applied in benchmarking of a numerical simulator.

Contents

Outline

The outline of this thesis is as follows:

Chapter 1-Introduction: In this chapter we give an introduction to the general concept of geothermal energy and look at the benefits and possible negative impacts of extracting this energy source. We also present the different processes of heat transfer in porous media, where we focus on natural convection and the occurrence of convection cells. Finally we describe how convection currents are important in geothermal fields and how convective cells might be affected by the presence of geological layers in the porous medium.

Chapter 2-Theory Concerning Fluid Flow in Porous Media: Basic definitions and concepts from fluid mechanics and reservoir engineering are introduced. Based on physical laws concerning fluid flow in porous media we establish the model equations needed to form a closed system. This system will serve as a framework for the description of natural convection. Assumptions are made, and the model therefore represents an idealized physical setting.

Chapter 3-Mathematical Model for Natural Convection: In this chapter we introduce the two-layer model and specify the boundary conditions required to solve the system. A stationary solution is found and perturbed to allow convection to occur. We non-dimensionalize the linearized equations and boundary conditions to end up with the final mathematical model used throughout the rest of the thesis.

Chapter 4-Linear Stability Analysis: The mathematical model developed in Chapter 3 is used to find the solutions of our system of equations, expressed in terms of the pressure and temperature. Further, we apply the boundary conditions to these solutions, which enable us to determine the criterion for onset of natural convection, stated through the

critical Rayleigh number.

Chapter 5-Results and Discussion: In this chapter the results from the linear stability analysis is presented and evaluated. The results include plots of the critical Rayleigh number as a function of the permeability contrast, which is compared with related results in previous literature.

Chapter 6-Conclusion: The final chapter gives a summary of this thesis together with conclusions from the analysis.

Chapter 1

Introduction

This thesis investigates natural convection in layered porous media, which is a central phenomenon in modelling of geothermal fields. In this chapter we give a short introduction to geothermal energy and present the most relevant environmental benefits and impacts of this resource. We explain how heat is transported through a porous medium and why convection is important for extraction of geothermal energy. Finally we introduce the concept of geological layering in subsurface porous media.

1.1 Geothermal Energy

The following presentation is mainly based on two books about geothermal energy by Kagel *et al.* [8] and Gupta and Roy [6], and the 2006 MIT report about the future of geothermal energy [20].

Geothermal energy is defined as the thermal energy stored in the Earth's crust. The heat originates from the creation of the Earth and from radioactive decay of isotopes. Since geothermal energy is a renewable and sustainable resource, it might provide an important contribution in meeting the world's growing energy needs. A large variety in systems for extracting the geothermal energy can be applied; fracturing of the ground, using open or closed systems, including numerous injecting and producing wells and the choice of carrier medium. The use of this energy source clearly has less negative impacts than many other resources. A deeper insight and a better understanding of geothermal systems will be crucial for future utilization.

One of the main benefits of geothermal energy is its constant availability. While many other renewable energy sources often rely on daily and seasonal

weather variations, geothermal energy is basically limitless and can be produced continuously. In addition to its reliability, geothermal energy also has several environmental benefits like the ability to operate almost emission-free and having a small land footprint, to mention some.

The extraction of geothermal energy may also have some negative impacts on the environment. These include the use of fresh water and land area, induced seismicity and emission of some greenhouse gases. As mentioned above, geothermal energy extraction virtually has no emissions. However, some emissions of greenhouse gases will be released from the subsurface during drilling and under production in open systems. These gases are mostly carbon dioxide (CO_2) and hydrogen sulphide (H_2S) which are present in the ground initially, and are not used in the extraction process. When comparing the amount of greenhouse gases emitted per produced megawatt-hour, a geothermal plant clearly releases much less than fossil-fueled power plants. See the MIT-report [20], Chapter 8.1, for further details.

The quality and potential of a geothermal resource vary widely from one location to another, as it depends on several regional geological properties. Some examples are the reservoir's permeability, porosity, heat conductivity, local heat production, vertical heat flow and the amount of fluid saturation. One of the most important factors to be considered is the temperature-depth relation. The temperature increases with depth towards the core of the Earth, where the temperature has the highest value. This increasing rate is called the temperature gradient or the geothermal gradient. A large temperature gradient is preferable in geothermal energy extraction because higher temperatures can be reached at lower depths. The areas with highest geothermal gradient are located at places where the crust is thin and at the boundaries of tectonic plates. These areas are limited and represent a minority of the land area on earth. If geothermal energy should compete as a future energy resource, it is important that the geothermal energy in areas of lower temperature gradient can be efficiently extracted in an economically feasible way. Knowledge about the state of heat transportation in the subsurface in these areas is therefore important when evaluating if a geothermal field is viable [6].

1.2 Heat Transfer in Porous Media

Heat transfer is the process where thermal energy is transported from a region of warmer temperature to a region of colder temperature. In general

there are four basic modes of heat transfer: conduction, convection, phase change and radiation [3]. In a porous medium, heat transfer is mainly due to conduction and convection, even though the two latter modes may also occur.

A small displacement of a molecule leads to a collision with the neighboring molecule, which results in an exchange of kinetic energy between them [2]. When heat diffuses through a solid or a stationary fluid in a porous medium this way, the mechanism is called *heat conduction*. Heat conduction has a smoothening effect on the temperature field, as the heat is always transferred from a region of higher temperature towards a region with lower temperature at a rate proportional to the temperature gradient.

Heat convection is when thermal energy is transferred with the movement of a fluid through the porous medium. The heat is carried with the fluid as it is moving, and the motion of molecules can either be in the form of random diffusion, advection or a combination of them. When the term 'convection' is used, it refers to the sum of both diffusive and advective transfer of heat.

There are two types of convection: forced convection and free/natural convection. Forced convection is the mechanism where external sources impose the movement of the fluid. Natural convection is when density differences due to variations in the temperature generate the fluid motion. Fluids that are heated will become less dense and rise. To make room for the rising fluid, the cooler fluid at the top moves. Being denser it will flow towards the bottom of the system, and the overall process results in a bulk fluid motion. Both forced and free convection may occur in a system at the same time, in which case we have mixed convection.

Often one form of heat transfer will be dominating in the subsurface, and the knowledge of this can give valuable information when characterizing a system. Even though both conduction and convection have important roles in the process of heat transportation, convection is the most efficient way of transferring heat in the Earth [6]. Hence, convection might have an important impact for production of geothermal energy.

1.3 Impact of Convection Cells for Production of Geothermal Energy

In a porous medium where there exists density differences in the fluid, heat transfer by convection may occur. The fluid flow in such a system is referred to as convection currents. A characteristic flow pattern formed by the convection currents is convection cells [2]. A convection cell is a repeating cycle were rising and falling fluid currents follow closed trajectories. Convection cells can be caused by natural-, forced- and mixed convection, and the process is very similar to the one described for natural convection in Section 1.2.

The mechanism in a convection cell is as follows: We assume that the system initially contains a stationary fluid, which is heated from below and cooled from above due to the geothermal gradient. When the density of the fluid varies with temperature, where the fluid is lighter at warmer temperatures, the lower fluid will be lighter than the fluid above. If there is a small disturbance or perturbation to this stationary phase, it may cause the warmer fluid to rise. As the fluid is rising it loses some heat because of direct energy exchange with the cooler surroundings located closer to the ground surface. The fluid continues to rise and turn colder, but at some point it will become denser than the fluid beneath it, which is still rising. Since it cannot flow through the fluid below it has to move to the side, allowing the lighter fluid to pass. Eventually the force acting downwards will be larger than the rising force, and the fluid starts to descend. While descending the fluid is heated up again. When it reaches the starting position, the cycle is repeated. See Figure 1.1 for a schematic sketch of convection cells.

As mentioned in Section 1.1, when evaluating the quality and potential of a specific location for a new geothermal power plant, a large temperature gradient and vertical heat flow are desirable. Based on analysis from several geothermal wells at Soultz-sous-Forêts, France, it is assumed that convection cells have a significant impact on the geothermal gradient [17]. This impact might include both positive and negative effects on the temperature field. If the location of the cell is beneficial, convection may contribute to an even better efficiency of heat extraction by retrieving heat far away from the geothermal well. The amount of extra heat transfer depends on the velocity and horizontal extent of the convection cell, which is again depending on, and affected by, the different geological layers present in the subsurface.

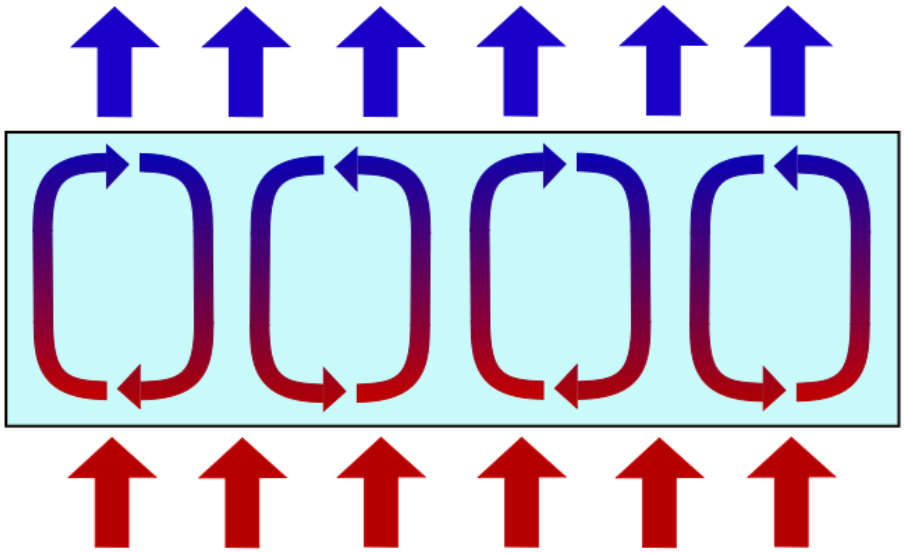

Figure 1.1: Convection cells in a porous medium which is heated from below and cooled from above. The figure is borrowed from [4].

1.4 Layering in Porous Media

Most naturally occurring porous media present in the subsurface contain layers. In a geothermal context, it is important to consider layering within the medium, as it causes spacial and directional variations in the ground [13]. The interfaces between each layer generally allows for fluid to flow through [18]. The movement of materials through such a medium will be affected by the number of layers, the size of each layer and the parameters within each layer.

Many authors have studied convection in single-layer porous media, but fewer have considered the case of a multi-layered medium. Studies of the latter have shown that the presence of layers can influence the convective patterns and the criterion for onset of convection. A common result is that a significant difference in the flow rate between two neighbouring layers is required for a transition from large-scale convection occurring throughout both layers, to local convection confined to one of the layers [10]. These different cases are demonstrated in Figure 1.2.

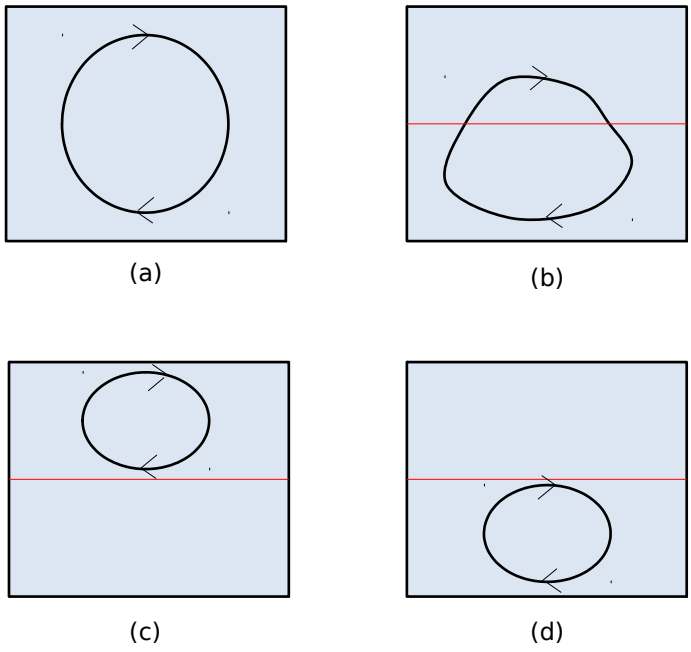

Figure 1.2: Illustration of convection in a layered porous medium. The red line defines the interface between the two layers. Picture (a) represents a homogeneous porous medium, (b) illustrates large-scale convection and picture (c) and (d) show cases of local convection.

Since the temperature field in the subsurface will be affected by the presence of convection cells in layered porous media, knowledge about their initial position is highly valued in the geothermal industry. This thesis presents useful results, as they indicate whether natural convection is present in the subsurface. Because we find the criterion for onset of convection, the model may also serve a purpose for validation of a numerical code in a simulation model. The results can be used to check if the numerical code gives correct information about the onset of convection, and this way our results can be applied in benchmarking the code. Even though the following chapters introduce an analysis based on an idealized physical setting, the model is still relevant.

Chapter 2

Theory Concerning Fluid Flow in Porous Media

The understanding of fluid flow in the subsurface is important when dealing with extraction of geothermal energy. To investigate the movement of a fluid through a porous medium, knowledge from fluid mechanics and reservoir engineering is of high relevance. In this chapter we introduce the basic definitions, concepts and equations needed to make the analysis governing natural convection in a porous medium, and these will be used throughout the thesis. The theory presented in this chapter is mainly based on books of Bear [2], Nield and Bejan [14] and Nordbotten and Celia [15].

2.1 Porous Matrix Properties

There are several examples of porous materials, such as soil, skin, sand, concrete, ceramics and bedrocks. The straight forward way to describe a porous medium is to view it as a material containing holes. The solid part is often referred to as the 'skeleton' or the 'matrix', while the rest of the material is generally known as 'the pore space' or 'the void space'. This definition is somehow rather weak, since a solid with isolated pores also would fit under this category, even though it is normally not considered to be a porous medium. When studying flow in porous media we are interested in the case where a fluid can move continuously through the medium. By restricting our definition of a porous medium to include pores that are interconnected, we have a better definition for our purpose of investigations. This way, bedrocks represent porous media because they contain pathways where a fluid, for example water, can flow through. An irregularity in the pattern of the pathways exists, as bedrocks contain different geological layers where

the size and shape of the layers depend on when, where and how they were created.

2.1.1 Representative Elementary Volume

An irregularity with respect to the size and shape of the pores and the distribution of the voids throughout the material exist in all porous media. This irregularity gives rise to a very complex network within the medium. To describe the flow through the pores mathematically, we consider this complex pattern as random variations with a clearly defined average. Each property is therefore representing an average over a certain volume. This volume is called the '*representative elementary volume*' (REV). The REV has to include both solid and pores to give any valid information about the medium. The size should be large enough to represent a mean global property and to make sure that the effect of fluctuations between pores is neglectable. On the other hand, it needs to be small enough to keep the properties local and to enable an approximation of the properties using continuous functions [2]. The REV contains voids that form interconnected pathways, but may also consist of isolated pores and dead- ends where the fluid flow is limited, see Figure 2.1.

2.1.2 Porosity

When describing a representative elementary volume, the *porosity* ϕ of the porous matrix is often used. Porosity is defined as the ratio of the volume of pores V_P present in the REV to the total volume V_T,

$$\phi = \frac{V_P}{V_T}.$$

This porosity is defined as the 'total' or 'absolute' porosity, since it includes all the voids in the concerning volume. When describing the flow of a fluid in a porous medium it is only the interconnected voids that are interesting, as there is no continuous flow within the isolated or blind-way pores. It is therefore natural to introduce the concept of *effective porosity* ϕ_E, defined as the fraction of the volume in the REV occupied by interconnected voids (also known as the effective pore space) V_{EP} and the total volume V_T; that is,

$$\phi_E = \frac{V_{EP}}{V_T}.$$

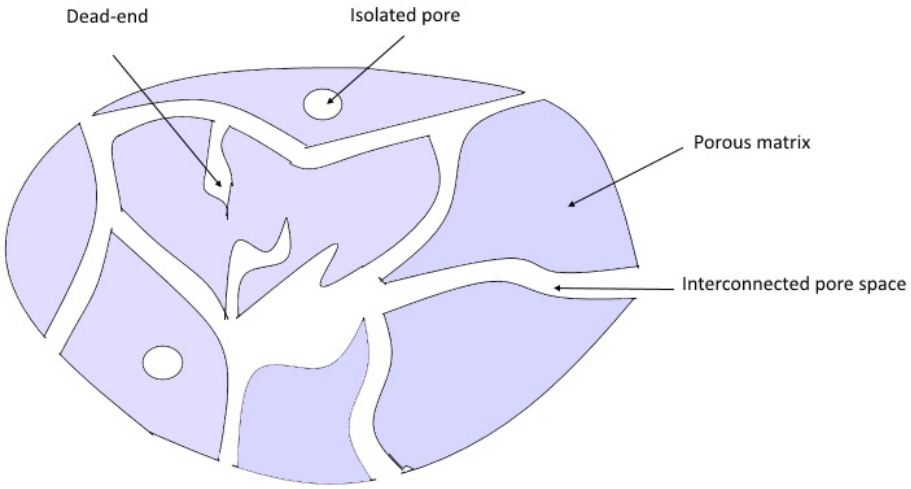

Figure 2.1: A porous medium containing interconnected voids, isolated pores and dead-ends.

We will only make use of the effective porosity in our calculations. The term 'porosity' is used throughout the rest of this thesis, meaning the effective porosity. For simplicity we also omit writing ϕ_E, and use ϕ instead.

2.2 Fluid Properties

The void space in the porous medium allows for one or several fluids to flow through. If only one fluid phase is present in the pore space it is referred to as single-phase flow. Otherwise it is called multiphase-flow. In this thesis we have a single fluid occupying the void space. We consider water as the fluid phase and assume that all pores are fully saturated.

2.2.1 Density

Density describes the distribution of mass in space. The fluid density ρ is defined as the mass of the fluid per unit volume, and has SI-unit kg/m^3. Generally the density varies with pressure P and temperature T, in which case the relation between them can be expressed using an equation of state:

$$\rho = \rho(P, T).$$

In our analysis we will assume the density to be independent of pressure. Further, we look at the case where the density is linearly dependent on temperature, written mathematically as

$$\rho = \rho_0[1 - \beta_g(T - T_0)], \tag{2.1}$$

where $\rho = \rho_0$ at some reference temperature T_0 and β_g is a constant called the thermal expansion coefficient. This constant is a positive number since water becomes less dense for increasing temperatures [11].

We will use the Boussinesq approximation in this thesis. The approximation states that unless multiplied with the gravity acceleration g, the density differences are so small that we can neglect them in our calculations [14]. The combination of the Boussinesq approximation and equation (2.1) shows that the thermal expansion coefficient β_g can be neglected in all cases where it is not multiplied with g.

2.2.2 Viscosity

When shear stress is applied to a fluid, it will give rise to a deformation. Under the presence of such a force the fluid will continue to deform, and we refer to this phenomenon as the fluid flow. The flow rate depends on the *viscosity* μ of the fluid, which describes the fluid's ability to resist any deformation when it is moving. The SI-unit of viscosity is kg/ms. One way to visualize the concept of viscosity is by thinking of fluids as having different 'thickness'. The higher the viscosity, the thicker the fluid. Honey is an example of a 'thick' fluid with high resistance to flow, while water represents a 'thin' fluid which flows easily due to low viscosity.

In reality, the viscosity μ and the thermal expansion coefficient β_g may depend on pressure and temperature. We assume both to be constant for simplicity.

2.3 Model Equations

In the remaining of this chapter, we formulate the governing equations relevant for natural convection.

2.3.1 Darcy's Law and Permeability

When describing the fluid flow in a porous medium, Darcy's law is one of the most important equations. In 1856 Henry Darcy published his work where he investigated the water flow through a horizontal layer of sand. He used different types of sand as porous medium, and performed several experiments. Based on important observations he was able to predict the amount of water that would flow through his domain. He noticed that the volumetric flow rate of water q was proportional to the cross section area A of the layer and the pressure drop ΔP over the sand sample, but inversely proportional to the layer's length L. These key observations lead to the following important equation:

$$q = \hat{K} A \frac{\Delta P}{L}, \tag{2.2}$$

where $\hat{K}$ is the coefficient of proportionality, often referred to as the hydraulic conductivity. Since the hydraulic conductivity depends on both the porous medium and the fluid, it indicates how easy a fluid flows through a porous medium. The relation is as follows:

$$\hat{K} = K \frac{\gamma_w}{\mu}. \tag{2.3}$$

Here $\gamma_w = \rho g$ is the specific weight of the fluid, μ is the fluid's viscosity and K represent the permeability of the porous matrix.

Permeability is a property of high importance when discussing porous media. It is a measure of how easily a fluid can flow through the void space of the medium. The larger the permeability K, the better the porous medium can transmit fluid. A unit of the permeability K is Darcy, which equals $0.987 \cdot 10^{-12}\mathrm{m}^2$. The permeability might vary with space and direction. If a property like the permeability changes with the spacial position, the system is called heterogeneous and we write $K = K(x, y, z)$. If it is spatially uniform, that is independent of position, we have a homogeneous system. When the relation between flow and pressure drop depends on the flow direction, the permeability is anisotropic. In such a system the permeability is expressed as a tensor $\mathbf{K}$. Conversely, a domain with no directional differences is an

isotropic system.

In this thesis we assume that the porous medium is layered, where each layer is homogeneous and isotropic. The properties of the porous matrix are thus constant scalars throughout all layers. By using the assumption that each layer in our domain is homogeneous and isotropic, and by writing equation (2.2) in differential form with equation (2.3) inserted, we get the modern form of Darcy's law:

$$\mathbf{v} = -\frac{K}{\mu}(\nabla P + \rho g \mathbf{k}). \tag{2.4}$$

Here, g is the gravitational acceleration, $\mathbf{k}$ is a vertical unit vector which points upwards and $\mathbf{v}$ is the Darcy velocity. An important notification is that the Darcy velocity $\mathbf{v}$ represents the average fluid velocity over the total volume V_T. By averaging the fluid velocity over the volume of fluid V_f only, we will get the intrinsic average velocity $\mathbf{V}$. This velocity is related to the Darcy velocity through the Dupuit-Forchheimer relationship [14]:

$$\mathbf{v} = \phi \mathbf{V}. \tag{2.5}$$

Darcy's law is only valid when there is one phase present in the void space. Another validation criterion is that the fluid does not react in any way with the medium. Finally, Darcy's law is applicable when the velocity of the fluid is small. The term 'small' is vague, but the typical velocities for most cases of fluid flow in a porous medium is in the scope of Darcy's law, typically cm/hour or less [16]. A fluid velocity beneath this 'limit' causes friction between the pore walls and the fluid to dominate the system. Too large speed may cause turbulence, in which case Darcy's law does no longer apply. In this thesis we assume that all these criteria are fulfilled.

2.3.2 Mass Conservation

A second important equation when describing the transport of fluid through a porous medium is the mass conservation. This equation states that any change of mass inside a given volume Ω equals the sum of mass entering or leaving the volume through the boundary $\partial\Omega$ and the mass appearing inside the volume through sources or sinks, which are not associated with the boundary; that is,

$\{\text{Change of mass}\} = \{\text{Change due to flux}\} + \{\text{Change due to sources/sinks}\}.$

This can be written mathematically as follows:

$$\int_{\Omega} \frac{dm_v}{dt} dV = -\int_{\partial\Omega} \mathbf{f} \cdot \mathbf{n} dS + \int_{\Omega} q_m dV. \tag{2.6}$$

Here m_v is the mass per volume, $\mathbf{f}$ is the mass flux vector, $\mathbf{n}$ is the outward unit normal and q_m represents any sources or sinks within the volume, see Figure 2.2.

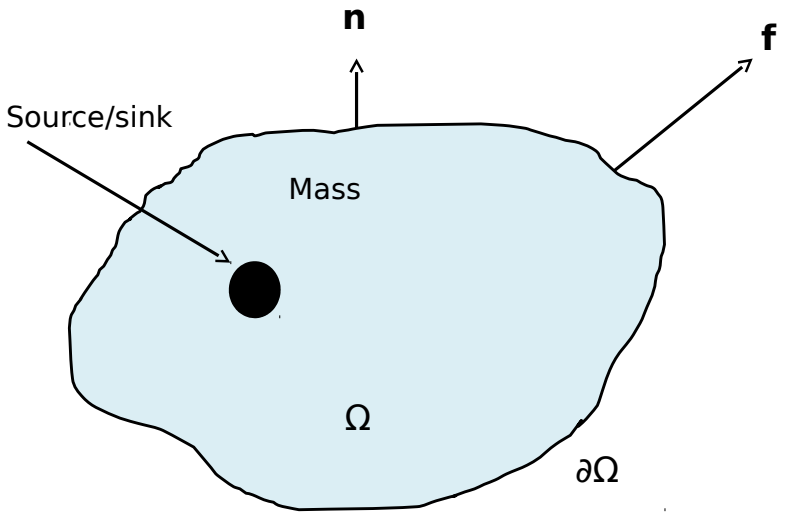

Figure 2.2: A domain Ω with boundary $\partial\Omega$, a fixed mass m_v, outward unit normal $\mathbf{n}$ and flux vector $\mathbf{f}$.

If we apply the divergence theorem,

$$\int_{\partial\Omega} \mathbf{f} \cdot \mathbf{n} dS = \int_{\Omega} \nabla \cdot \mathbf{f} dV,$$

to the flux term in equation (2.6), assume that we have no sources or sinks in our domain and use the fact that the integrand of all terms are continuous,

we get:

$$\frac{dm_v}{dt} + \nabla \cdot \mathbf{f} = 0. \tag{2.7}$$

Since we are working with single-phase flow, we set $m_v = \rho\phi$ and $\mathbf{f} = \rho\mathbf{v}$ into equation (2.7), which becomes

$$\phi\frac{\partial\rho}{\partial t} + \nabla \cdot (\rho\mathbf{v}) = 0.$$

Due to the application of Boussinesq approximation mentioned in Subsection 2.2.1, we can remove all the density differences that are not multiplied with the gravity acceleration. The mass conservation equation then reads

$$\nabla \cdot \mathbf{v} = 0. \tag{2.8}$$

2.3.3 Energy Conservation

A volume consisting of porous medium and a fluid will retain conservation of energy due to the first law of thermodynamics. Since energy cannot be created or destroyed, only transformed, the first law states that the total energy within such a system equals the energy entering the domain minus the energy leaving. This principle gives rise to an equation of energy conservation in porous media, which we include in our model.

When studying porous media, it is clear that conduction and convection are responsible for most of the energy transport. The conductive heat flux through the solid can be written as $-k_s\nabla T_s$. Here k is the thermal conductivity, T is the temperature and the subscript s implies solid. The net rate of heat conduction into a unit volume of the solid is given by applying the divergence operator to the heat flux term, which becomes $\nabla \cdot (k_s\nabla T_s)$.
Similarly, the net rate of heat conduction into a unit volume of the fluid is $\nabla \cdot (k_f\nabla T_f)$, where f refers to the fluid phase. The energy transfer caused by convection is related to the movement of the fluid. The total rate of change of thermal energy due to fluid transport is $(\rho c_p)_f\mathbf{V} \cdot \nabla T_f$. In this expression, V is the instrinsic velocity and c_p is the specific heat at constant pressure of the fluid. Applying the Dupuit-Forchheimer relationship (2.5), assuming no phase changes in the system and adding the terms, we get [14]

$$\phi(\rho c_p)_f\frac{\partial T_f}{\partial t} + (\rho c_p)_f\mathbf{v} \cdot \bigtriangledown T_f = \phi\nabla \cdot (k_f\nabla T_f) + \phi q_f, \tag{2.9}$$

$$(1-\phi)(\rho c)_s \frac{\partial T_s}{\partial t} = (1-\phi)\nabla \cdot (k_s \nabla T_s) + (1-\phi)q_s. \tag{2.10}$$

Equation (2.9) and (2.10) represent the conservation of energy equation for the fluid and the solid respectively. Here, c is the specific heat of the solid, while q is the heat production per unit volume.

We assume local thermal equilibrium. This means that the temperature of the solid and fluid is the same, so $T_s = T_f = T$. We will also assume that there is no heat production within our system, and set the production terms equal to zero. If we add equations (2.9) and (2.10) we obtain an overall equation for energy conservation;

$$(\rho c)_m \frac{\partial T}{\partial t} + (\rho c_p)_f \mathbf{v} \cdot \nabla T = \nabla \cdot (k_m \nabla T), \tag{2.11}$$

where

$$(\rho c)_m = (1-\phi)(\rho c)_s + \phi(\rho c_p)_f,$$

$$k_m = (1-\phi)k_s + \phi k_f.$$

Here, $(\rho c)_m$ is the overall heat capacity per unit volume and k_m is the overall thermal conductivity [14]. To ease the notation we will write k instead of k_m throughout the rest of this thesis.

Chapter 3

Mathematical Model for Natural Convection

In Chapter 2 we found the following three equations:

Darcy's law,

$$\mathbf{v} = -\frac{K}{\mu}(\nabla P + \rho g \mathbf{k}), \tag{3.1}$$

the mass conservation equation,

$$\nabla \cdot \mathbf{v} = 0, \tag{3.2}$$

and the energy conservation equation,

$$(\rho c)_m \frac{\partial T}{\partial t} + (\rho c_p)_f \mathbf{v} \cdot \nabla T = \nabla \cdot (k \nabla T). \tag{3.3}$$

When including the equation of state for the fluid density (2.1), these form a closed system of equations where $\mathbf{v}$, P and T are the unknowns.

In this thesis we make use of cylindrical coordinates. The Darcy velocity vector $\mathbf{v}$ then becomes

$$\mathbf{v} = v_r \mathbf{e_r} + v_\theta \mathbf{e}_\theta + v_z \mathbf{k}, \tag{3.4}$$

where $\mathbf{e_r}$ and $\mathbf{e}_\theta$ are unit vectors in the radial and azimuthal direction.

The gradient operator is given by

$$\nabla T = \frac{\partial T}{\partial r}\mathbf{e_r} + \frac{1}{r}\frac{\partial T}{\partial \theta}\mathbf{e}_\theta + \frac{\partial T}{\partial z}\mathbf{k},$$

the divergence operator is defined as

$$\nabla \cdot \mathbf{v} = \frac{1}{r}\frac{\partial(rv_r)}{\partial r} + \frac{1}{r}\frac{\partial v_\theta}{\partial \theta} + \frac{\partial v_z}{\partial z},$$

and the curl operator reads

$$\nabla \times \mathbf{v} = (\frac{1}{r}\frac{\partial v_z}{\partial \theta} - \frac{\partial v_\theta}{\partial z})\mathbf{e_r} + (\frac{\partial v_r}{\partial z} - \frac{\partial v_z}{\partial r})\mathbf{e}_\theta + \frac{1}{r}(\frac{\partial(rv_\theta)}{\partial r} - \frac{\partial v_r}{\partial \theta})\mathbf{k}.$$

3.1 The Two-Layer Model

Our domain is a porous medium between two vertical, coaxial cylinders, as seen in Figure 3.1. The radius of the inner cylinder is R_I and the outer cylinder has radius R_O. The porous medium consists of two layers with different permeability, K_1 and K_2, different thermal conductivities, k_1 and k_2 and different heights, h_1 and h_2. The total height is $h = h_1 + h_2$. The cylinders are heated from below and cooled from above, with temperatures T_w and T_c respectively.

We chose to study a two-layer model for simplicity, but our method is also suitable for a multi-layered system. Due to the fact that two layers are present, our equations (3.1)-(3.3) apply separately for each of them, where $\mathbf{v}_1$, P_1 and T_1 are defined for $0 \leq z \leq h_1$, and $\mathbf{v}_2$, P_2 and T_2 are defined for $h_1 \leq z \leq h_1 + h_2$.

For each layer $i = \{1, 2\}$, Darcy's law becomes

$$\mathbf{v_i} = -\frac{K_i}{\mu}(\nabla P_i + \rho g \mathbf{k}), \tag{3.5}$$

the mass conservation equation is

$$\nabla \cdot \mathbf{v_i} = 0, \tag{3.6}$$

and the energy conservation equation reads

$$(\rho c)_m \frac{\partial T_i}{\partial t} + (\rho c_p)_f \mathbf{v_i} \cdot \nabla T_i = \nabla \cdot (k_i \nabla T_i). \tag{3.7}$$

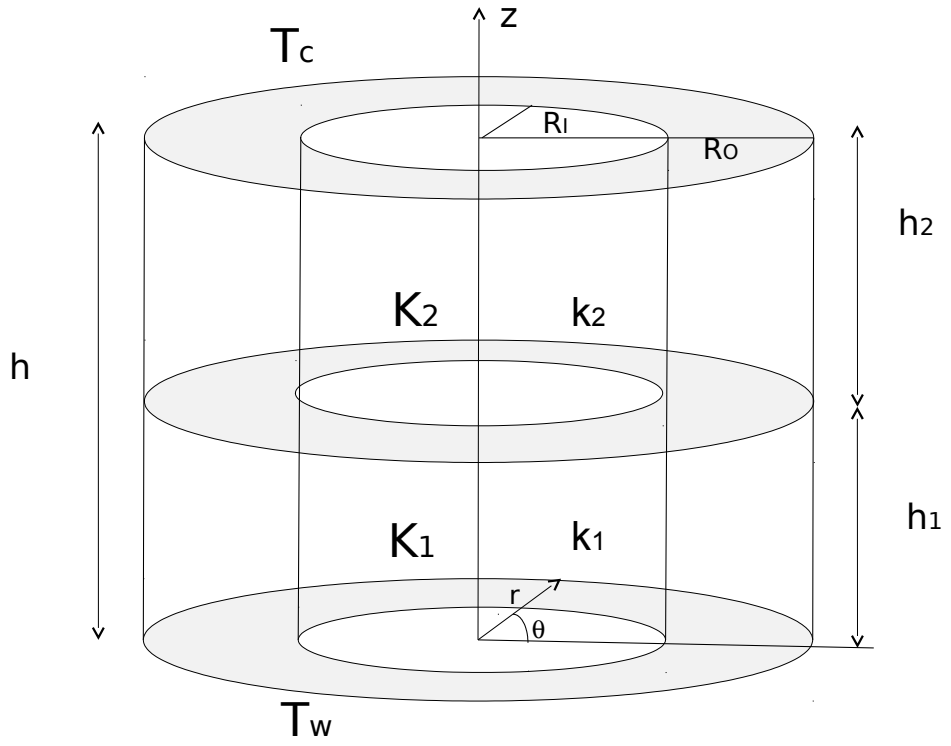

Figure 3.1: Two coaxial cylinders with radius R_I and R_O, and height h. A porous medium consisting of two layers of different permeability and conductivity is located between the cylinders. These layers have height h_1 and h_2.

To solve the above system, boundary conditions needs to be specified. By assuming 2π-periodicity in the azimuthal direction, it is not necessary to define explicit boundary conditions there. Boundary conditions are required at the top and bottom and in the vertical sidewalls of both cylinders, in addition to continuity conditions at the interface between the two layers of the porous medium.

Both the top and bottom of the cylinders are assumed to be impermeable and perfectly heat conducting. Impermeable means that no fluid can flow through, which mathematically reads

$$\begin{aligned} v_{z,1} &= 0 \quad \text{at } z = 0, \\ v_{z,2} &= 0 \quad \text{at } z = h. \end{aligned} \tag{3.8}$$

Perfectly heat conducting means that the temperature is held constant at all times. This can be formulated as

$$\begin{aligned} T_1 &= T_w \quad \text{at } z = 0, \\ T_2 &= T_c \quad \text{at } z = h. \end{aligned} \tag{3.9}$$

We consider the sidewalls to be impermeable; that is,

$$v_{r,i} = 0 \quad \text{at } r \in \{R_I, R_O\}, \tag{3.10}$$

and insulated; that is,

$$\frac{\partial T_i}{\partial r} = 0 \quad \text{at } r \in \{R_I, R_O\}. \tag{3.11}$$

Insulated sidewalls imply that the temperature gradient over the vertical boundaries is zero, so that there are no heat flow over the sidewalls.

At the interface between the layers, continuity in temperature, pressure, vertical flow and vertical heat flux is assumed.

Continuity in temperature is written as

$$T_1|_{z=h_1} = T_2|_{z=h_1}\,, \tag{3.12}$$

while continuity in pressure is described through

$$P_1|_{z=h_1} = P_2|_{z=h_1}\,. \tag{3.13}$$

The continuity in vertical flow reads

$$v_{z,1}|_{z=h_1} = v_{z,2}|_{z=h_1}\,, \tag{3.14}$$

and continuity in heat flux can be expressed as

$$k_1 \frac{\partial T_1}{\partial z}\bigg|_{z=h_1} = k_2 \frac{\partial T_2}{\partial z}\bigg|_{z=h_1}\,. \tag{3.15}$$

3.2 The Stationary Solution

To study the onset of convection in our layered porous medium, we first need to find the stationary solution. The equations (3.5) - (3.7) together with the boundary conditions (3.8)-(3.15) have the following steady-state solution:

$$T_{S,1} = T_w - (T_w - T_c)\frac{k_2}{k_2h_1 + k_1h_2}z, \quad 0 \le z \le h_1,$$

$$T_{S,2} = T_w - (T_w - T_c)\Big(\frac{h_1(k_2 - k_1)}{k_2h_1 + k_1h_2} + \frac{k_1}{k_2h_1 + k_1h_2}z\Big), \quad h_1 \le z \le h_1 + h_2,$$

$$\begin{aligned} \mathbf{v}_{S,1} &= 0, && 0 \le z \le h_1, \\ \mathbf{v}_{S,2} &= 0, && h_1 \le z \le h_1 + h_2, \end{aligned}$$

$$P_{S,1} = \rho_0 g(\beta T_w - T_0 - 1)z - \rho_0 g\beta(T_w - T_c)\frac{k_2z^2}{2(k_2h_1 + k_1h_2)} + P_{0,1}, \quad 0 \le z \le h_1,$$

$$\begin{aligned} P_{S,2} = {} & \rho_0 g[\beta T_w - (T_w - T_c)\frac{h_1(k_2 - k_1)}{k_2h_1 + k_1h_2} - \beta T_0 - 1]z - \\ & \rho_0 g\beta(T_w - T_c)\frac{k_1z^2}{2(k_2h_1 + k_1h_2)} + P_{0,2}, \qquad h_1 \le z \le h_1 + h_2. \end{aligned}$$

Here, the constants $P_{0,1}$ and $P_{0,2}$ are defined such that continuity in pressure is fulfilled. In the stationary solution, heat flow is only due to conduction. Since we are interested in the onset of convection in our analysis, we need to perturb this solution.

3.3 Perturbation and Linearization of the Equations

A small perturbation applied to the conduction solution may cause convection to occur. A perturbation added to the system can be written as follows:

$$T_i = T_{S,i} + T_i', \quad \mathbf{v}_i = \mathbf{v}_{S,i} + \mathbf{v}_i' \text{ and } \quad P_i = P_{S,i} + P_i'.$$

Here T_i', $\mathbf{v}_i'$ and P_i' represent small quantities. Following the standard stability analysis procedure, we substitute these into our system of equations (3.5)-(3.7) and neglect all nonlinear terms. Since we are only concerned with the onset of convection, we also neglect the time derivative. Our model turns into equations for the perturbed quantities T_i', $\mathbf{v}_i'$ and P_i';

Darcy's law becomes

$$\mathbf{v}_i' = -\frac{K_i}{\mu}(\nabla P_i' - \rho_0 g\beta T_i'\mathbf{k}) \quad \text{for } i \in \{1, 2\}, \tag{3.16}$$

mass conservation is

$$\nabla \cdot \mathbf{v}_i{}' = 0 \quad \text{for } i \in \{1, 2\}, \tag{3.17}$$

and the energy equations now read

$$\begin{aligned} -(\rho c)_f \mathbf{v}_{z,1}{}'(T_w - T_c)\frac{k_2}{k_2 h_1 + k_1 h_2} &= k_2 \nabla^2 T_1{}', \\ -(\rho c)_f \mathbf{v}_{z,2}{}'(T_w - T_c)\frac{k_1}{k_2 h_1 + k_1 h_2} &= k_1 \nabla^2 T_2{}'. \end{aligned} \tag{3.18}$$

The boundary conditions for the perturbed quantities are as follows:

At the top and bottom, we have that

$$\begin{aligned} v_{z,1}{}' &= 0 \quad \text{at } z = 0, \\ v_{z,2}{}' &= 0 \quad \text{at } z = h, \end{aligned} \tag{3.19}$$

$$\begin{aligned} T_1{}' &= 0 \quad \text{at } z = 0, \\ T_2{}' &= 0 \quad \text{at } z = h. \end{aligned} \tag{3.20}$$

Along the sidewalls, the conditions are

$$v_{r,i}{}' = 0 \quad \text{at } r \in \{R_I, R_O\}, \tag{3.21}$$

$$\frac{\partial T_i{}'}{\partial r} = 0 \quad \text{at } r \in \{R_I, R_O\}. \tag{3.22}$$

At the interface, continuity is described mathematically as

$$T_1{}'|_{z=h_1} = T_2{}'|_{z=h_1}, \tag{3.23}$$

$$v_{z,1}{}'|_{z=h_1} = v_{z,2}{}'|_{z=h_1}, \tag{3.24}$$

$$P_1{}'|_{z=h_1} = P_2{}'|_{z=h_1}, \tag{3.25}$$

$$k_1 \frac{\partial T_1{}'}{\partial z}\bigg|_{z=h_1} = k_2 \frac{\partial T_2{}'}{\partial z}\bigg|_{z=h_1}. \tag{3.26}$$

3.4 The Nondimensional Model

In our calculations, we are interested in how a small perturbation of the parameters might affect the onset of natural convection. Since a change of two different parameters might affect the system in the same way, doing so would not necessarily give any new information. To make sure this does not happen, we nondimensionalize all our equations. This way we only have a few nondimensional ratios of parameters to vary, which makes it easier to note how different ratios affect the solution.

The coordinate transform we use to nondimensionalize the equations is based on the coordinate transform by McKibbin and O'Sullivan in [11] and [12]. They state that it is convenient to nondimensionalize the variables differently in each layer. For each layer $i = 1, 2$, the nondimensional variables are defined in the following way:

$$r^* = \frac{r}{h}; \qquad {Z_i}^* = \frac{z - h_{i-1}}{h_i}; \quad {v_{r,i}}^* = \frac{{v_{r,i}}' h}{b_i \alpha_{f,i}}; \quad {v_{\theta,i}}^* = \frac{{v_{\theta,i}}' h}{b_i \alpha_{f,i}}; \quad {v_{z,i}}^* = \frac{{v_{z,i}}' h}{b_i \alpha_{f,i}};$$
$$T_i^* = \frac{T_i'}{\Delta T_i}; \quad P_i^* = \frac{P_i' K_i}{\mu b_i \alpha_{f,i}}.$$

Here, r is the radius and b_i is the ratio of the height of layer i to the total height; $b_i = \frac{h_i}{h}$. The height h_0 is defined as $h_0 = 0$. The thermal diffusivity is denoted $\alpha_{f,i}$ where $\alpha_{f,i} = \frac{k_i}{(\rho c_p)_f}$. The temperature drop across each layer is denoted by ΔT_i, where $T_1 = T_m - T_w$, $T_2 = T_c - T_m$ and T_m is the temperature at the interface. Note that we are now differentiating between the layers in the vertical direction, where Z_1 is a variable in layer 1 and Z_2 is a variable in layer 2. See Figure 3.2 for an overview of the dimensionless domain. The superscript $*$ indicates that the parameters have no dimension.

Substituting the dimensionless variables into our model of equations (3.16)-(3.18) and boundary conditions (3.19)-(3.26), and defining the operators

$${\nabla_{b,i}}^* = \frac{\partial}{\partial r^*} + \frac{1}{r^*}\frac{\partial}{\partial \theta} + \frac{1}{b_i}\frac{\partial}{\partial z^*},$$

$${\nabla_{b,i}}^{*2} = \frac{1}{r^*}\frac{\partial}{\partial r^*}\left(r^*\frac{\partial}{\partial r^*}\right) + \frac{1}{r^{*2}}\frac{\partial^2}{\partial \theta^2} + \frac{\partial^2}{\partial {z^*}^2},$$

give a nondimensional model.

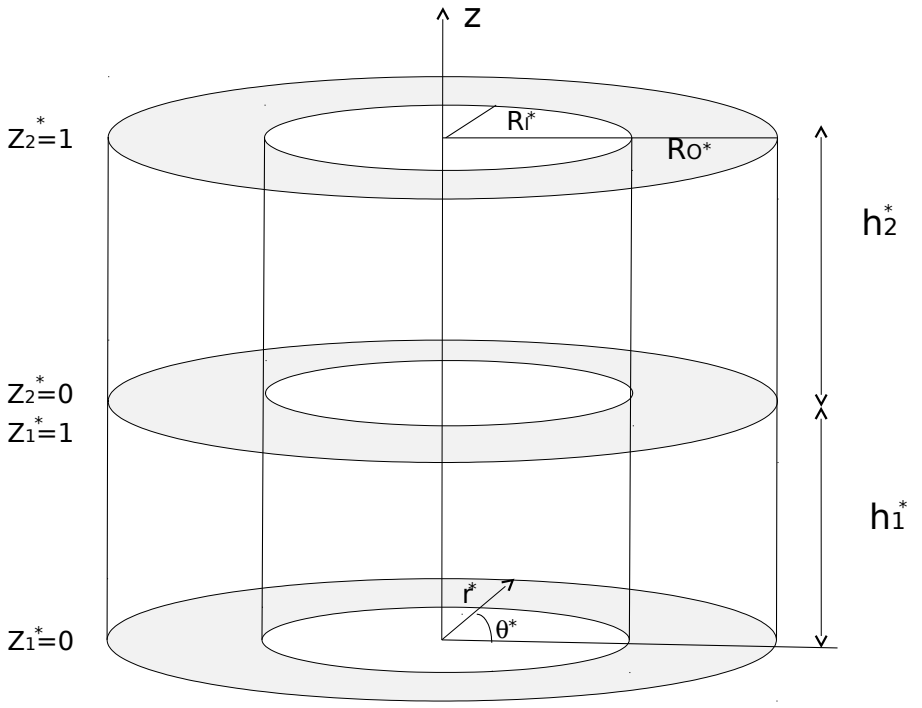

Figure 3.2: Domain with nondimensional variables.

For each layer, Darcy's law (3.16) becomes

$$\mathbf{v}_i{}^* = -\nabla_{b,i}{}^* P_i^* + \frac{Ra_i}{{b_i}^2} T_i{}^* \mathbf{k}, \quad 0 \leq Z_i^* \leq 1, \tag{3.27}$$

the mass conservation equation (3.17) is transformed into

$$\nabla_{b,i}{}^* \cdot \mathbf{v}_i{}^* = 0, \quad 0 \leq Z_i^* \leq 1, \tag{3.28}$$

and the energy conservation equations (3.18) read

$$-v_{z,i}{}^* = \nabla_{b,i}{}^{*2} T_i^*, \quad 0 \leq Z_i^* \leq 1. \tag{3.29}$$

In equation (3.27), Ra_i is a dimensionless number defined as $Ra_i = \frac{\rho_0 \beta g h_i K_i \Delta T_i}{\nu \alpha_{f,i}}$, which will be explained in detail in Section 3.5.

The dimensionless boundary conditions are as follows:

Impermeable and perfectly heat conducting top and bottom are written as

$$\begin{aligned} {v_{z,1}}^* &= 0 \quad \text{at } {Z_1}^* = 0, \\ {v_{z,2}}^* &= 0 \quad \text{at } {Z_2}^* = 1, \end{aligned} \tag{3.30}$$

$$\begin{aligned} {T_1}^* &= 0 \quad \text{at } {Z_1}^* = 0, \\ {T_2}^* &= 0 \quad \text{at } {Z_2}^* = 1, \end{aligned} \tag{3.31}$$

and impermeable and insulated sidewalls reads

$${v_{r,i}}^* = 0 \quad \text{at } r^* \in \{{R_I}^*, {R_O}^*\}, \tag{3.32}$$

$$\frac{\partial {T_i}^*}{\partial r^*} = 0 \quad \text{at } r^* \in \{{R_I}^*, {R_O}^*\}. \tag{3.33}$$

At the interface, continuity in temperature is now described through

$$\frac{b_1}{k_1}{T_1}^* \Big|_{{Z_1}^*=1} = \frac{b_2}{k_2}{T_2}^* \Big|_{{Z_2}^*=0}, \tag{3.34}$$

while continuity in vertical flow becomes

$$b_1 k_1 {v_{z,1}}^*|_{{Z_1}^*=1} = b_2 k_2 {v_{z,2}}^*|_{{Z_2}^*=0}. \tag{3.35}$$

The continuity in pressure is written as

$$\frac{b_1 k_1}{K_1}{P_1}^* \Big|_{{Z_1}^*=1} = \frac{b_2 k_2}{K_2}{P_2}^* \Big|_{{Z_2}^*=0}, \tag{3.36}$$

and continuity in heat flux now reads

$$\frac{\partial {T_1}^*}{\partial {Z_1}^*} \Big|_{{Z_1}^*=1} = \frac{\partial {T_2}^*}{\partial {Z_2}^*} \Big|_{{Z_2}^*=0}. \tag{3.37}$$

Because we use dimensionless parameters, the nondimensional height of the cylinders will be 1, the inner radius becomes ${R_I}^* = \frac{R_I}{h}$ and the outer radius transforms into ${R_O}^* = \frac{R_O}{h}$.

Since nondimensional variables are used throughout the rest of this thesis, we omit the superscript $*$. Unless specified in the text, all quantities are dimensionless.

3.5 The Rayleigh Number

The Rayleigh number, Ra_i, and Darcy number, Da_i, are important in association with natural convection. They appear from substitution of the dimensionless variables into the equations, and are given by

$$Ra_i = \frac{\rho_0 \beta_g g {h_i}^3 \Delta T_i}{\nu \alpha_{f,i}},$$

and

$$Da_i = \frac{K_i}{{h_i}^2},$$

where $\nu = \frac{\mu}{\rho_f}$ is the kinematic viscosity of the fluid. Note that all the parameters appearing in the fractions have dimension, but the resulting numbers are dimensionless. The Rayleigh number indicates which form of heat transfer, conduction or natural convection, is dominating in the domain, and is the traditional number related to a clear viscous fluid. The Darcy number gives information about the flow properties of the medium.

A multiplication of the Rayleigh number and Darcy number will introduce the Rayleigh-Darcy number;

$$Ra_i Da_i = Ra_i * Da_i = \frac{\rho_0 \beta_g g h_i K_i \Delta T_i}{\nu \alpha_{f,i}}. \tag{3.38}$$

This number is important concerning heat transport in porous media and depends on flow properties of the medium and fluid. Since we only use the Rayleigh-Darcy number in our calculations, we will refer to this number as the Rayleigh number, and use Ra_i as notation. This number is the one appearing in equation (3.27).

An indication of whether natural convection cells are present in a system can be given by comparing the Rayleigh number Ra_i to some constant $Ra_{c,i}$, called *the critical Rayleigh number*. This constant depends on the geometry and boundary conditions of the system. If the Rayleigh number is smaller than the critical value, conduction is the dominating form of heat transfer. If the Rayleigh number exceeds the critical value, heat transfer is primarily in the form of natural convection and convection cells might be present. For this reason, the critical Rayleigh number can be seen as a criterion for onset of convection in a system. A determination of this constant is of high importance when studying the heat transfer in different geometries and boundary conditions [6].

Chapter 4

Linear Stability Analysis

A description of onset of convection can be given by applying a linear stability analysis, but the method limits any attempt to describe convection at a later time. In a saturated porous medium the criterion for onset of natural convection depends on the domain's geometry and boundary conditions, and is expressed through the critical Rayleigh number. When a medium contains more than one layer, each layer will be described by its own critical Rayleigh number.

Several studies have previously been performed on the criterion for onset of convection in a homogeneous layer. Different aspects on the subject have been investigated by numerous authors. Horton and Rogers [7] and Lapwood [9] considered a uniform horizontal porous layer of infinite extent, which was heated from below and where the top and bottom surfaces were impermeable and perfectly heat conducting. Later, Bau and Torrance [1] studied an annular cylindrical cavity with insulated sidewalls and Bringedal *et al.* [5] did a similar analysis, where they also included heat conducting sidewalls. By letting the inner radius of the insulated sidewalls approach zero, Bringedal *et al.* [5] found that this boundary would not affect the onset of convection in a significant matter, which is also expected in our domain. The equations and analysis used in these previous studies can be extended to evaluate a multi-layered porous medium, and how the presence of layers affects the onset of convection. One such extension has been made by Masuoka *et al.* [10], who performed a stability analysis on the criterion for the onset of convection in a two-layer horizontal porous medium, where each layer had different permeabilities or conductivities. Similar transition of flow patterns were later found by McKibbin and O'Sullivan [11, 12], who extended the study to a multi-layered system. They investigated onset of convection and heat transfer in a system of several layers that were bounded below by an isothermal

and impermeable surface and above by an isothermal surface that could be either impermeable or at constant pressure. For both two- and three-layer systems, they used many different permeability ratios and layer thicknesses to evaluate the two-dimensional flow patterns at onset of convection and the associated critical Rayleigh numbers, cell widths and slope of the Nusselt number graph. Later, Rees and Riley [19] investigated the same problem in three dimensions.

To study the onset of convection in our model we will use separation of variables to find solutions for pressure and temperature in our system, and apply the boundary conditions to these expressions. This results in a system of equations from which the critical Rayleigh number can be found.

4.1 The System as Two Coupled Second-Order Differential Equations

In Chapter 3 we formulated a nondimensional model consisting of equations (3.27)-(3.29), together with the boundary conditions (3.30)-(3.37). Previous studies of natural convection in multi-layered media introduce a stream function to aid the solution, and solve the system in terms of the temperature and the stream function. This method only works for a system in two dimensions, and can therefore not be applied to our three-dimensional problem. Inspired by Rees *et al.* [18], who also investigated a three-dimensional case, we found it appropriate to solve our governing equations in terms of the temperature and pressure, hence we seek for equations in T and P only. By applying the divergence operator on Darcy's law (3.27), the left hand side can be set to zero using the mass conservation equation (3.28). This leads to the following equation:

$$\nabla_{b,i}{}^2 P_i = \frac{Ra_i}{{b_i}^3} \frac{\partial T_i}{\partial Z_i}. \tag{4.1}$$

By evaluating Darcy's law (3.27) in the vertical direction, we can use the energy conservation equation (3.29) to replace $v_{z,i}$ on the left side with $-\nabla_{b,i}{}^2 T_i$. This leads to our second equation in T and P, given by

$$\frac{1}{b_i} \frac{\partial P_i}{\partial Z_i} - \frac{Ra_i}{{b_i}^2} T_i = \nabla_{b,i}{}^2 T_i. \tag{4.2}$$

These two coupled second-order differential equations, one pair for each layer, together with the boundary conditions (3.30)-(3.37), now represent our model.

Since equation (4.1) and (4.2) are stated in terms of T and P, we also want the boundary conditions written in the same variables. We therefore need to rewrite the three boundary conditions (3.30), (3.32) and (3.35).

An evaluation of Darcy's law (3.27) in the vertical direction combined with boundary condition (3.31), gives us (3.30) in terms of P:

$$\begin{aligned} \frac{\partial P_1}{\partial Z_1} &= 0 \quad \text{at } Z_1 = 0, \\ \frac{\partial P_2}{\partial Z_2} &= 0 \quad \text{at } Z_2 = 1. \end{aligned} \tag{4.3}$$

Rewriting (3.32) is done by evaluating Darcy's law (3.27) in the radial direction. Since only the first term on the right hand side depends on the radius, this boundary condition becomes

$$\frac{\partial P_i}{\partial r} = 0 \quad \text{at } r \in \{R_I, R_O\}. \tag{4.4}$$

For the last boundary condition we can make direct use of the energy conservation equation (3.29) to obtain

$$b_1 k_1 \nabla_{b,1}{}^2 T_1 \big|_{Z_1=1} = b_2 k_2 \nabla_{b,2}{}^2 T_2 \big|_{Z_2=0}. \tag{4.5}$$

4.2 Solutions for Pressure and Temperature in the System

We now have the two coupled second-order differential equations (4.1) and (4.2) together with the boundary conditions (3.31), (3.33), (3.34), (3.36), (3.37) and (4.3) - (4.5). We can solve this system by using separation of variables. For details on how to do this, we refer to Appendix A.

The solutions we find in terms of pressure P and temperature T are as follows:

$$P_1(r,\theta,Z_1) = \Big[A_n J_n(\tau r) + B_n Y_n(\tau r)\Big]\cos(n\theta)F_1(Z_1), \tag{4.6}$$

$$P_2(r,\theta,Z_2) = \Big[A_n J_n(\tau r) + B_n Y_n(\tau r)\Big]\cos(n\theta)F_2(Z_2), \tag{4.7}$$

$$T_1(r,\theta,Z_1) = \Big[A_n J_n(\tau r) + B_n Y_n(\tau r)\Big]\cos(n\theta)G_1(Z_1), \tag{4.8}$$

$$T_2(r,\theta,Z_2) = \Big[A_n J_n(\tau r) + B_n Y_n(\tau r)\Big]\cos(n\theta)G_2(Z_2). \tag{4.9}$$

Here, n is a positive integer, A_n and B_n are constants, J_n and Y_n are Bessel functions of order n and of first and second kind, and τ is a wavenumber. The expressions for $F_1(Z_1)$, $F_2(Z_2)$, $G_1(Z_1)$ and $G_2(Z_2)$ are found by solving the system of coupled ordinary differential equations appearing in the vertical direction. The solution contains eigenvalues and their corresponding eigenvectors, from which $F_i(Z_i)$ and $G_i(Z_i)$ are composed. Owing to the possibility that some of the eigenvalues might be a complex number, the expressions in the vertical direction depends on these possible outcomes.

The eigenvalues are defined as

$$\beta_i = \sqrt{\tau^2 {b_i}^2 + \tau b_i \sqrt{Ra_i}}$$

and

$$\gamma_i = \sqrt{\tau^2 {b_i}^2 - \tau b_i \sqrt{Ra_i}},$$

when γ_i is a real number, or

$$\gamma_{i,Im} = \sqrt{\tau b_i \sqrt{Ra_i} - \tau^2 {b_i}^2},$$

when γ_i is a complex number, where $Re(\gamma_i) = 0$, $Im(\gamma_i) = \gamma_{i,Im}$.

By using these eigenvalues and their corresponding eigenvectors, the expressions for $F_i(Z_i)$ and $G_i(Z_i)$ are defined in the following way:

$$
\begin{aligned}
F_i(Z_i) &= C_{1,i}e^{\beta_i Z_i} + C_{2,i}e^{-\beta_i Z_i} + C_{3,i}e^{\gamma_i Z_i} + C_{4,i}e^{-\gamma_i Z_i},\\
G_i(Z_i) &= C_{1,i}\frac{\beta_i(\tau {b_i}^2\sqrt{Ra_i} - b_i Ra_i)}{(\tau^2 {b_i}^2 - Ra_i)Ra_i}e^{\beta_i Z_i} - C_{2,i}\frac{\beta_i(\tau {b_i}^2\sqrt{Ra_i} - b_i Ra_i)}{(\tau^2 {b_i}^2 - Ra_i)Ra_i}e^{-\beta_i Z_i}\\
&\quad - C_{3,i}\frac{\gamma_i(\tau {b_i}^2\sqrt{Ra_i} + b_i Ra_i)}{(\tau^2 {b_i}^2 - Ra_i)Ra_i}e^{\gamma_i Z_i} + C_{4,i}\frac{\gamma_i(\tau {b_i}^2\sqrt{Ra_i} + b_i Ra_i)}{(\tau^2 {b_i}^2 - Ra_i)Ra_i}e^{-\gamma_i Z_i},
\end{aligned}
\tag{4.10}
$$

when γ_i is a real number, and

$$
\begin{aligned}
F_i(Z_i) &= C_{1,i}e^{\beta_i Z_i} + C_{2,i}e^{-\beta_i Z_i} + C_{3,i}\cos(\gamma_{i,Im}Z_i) + C_{4,i}\sin(\gamma_{i,Im}Z_i),\\
G_i(Z_i) &= C_{1,i}\frac{\beta_i(\tau {b_i}^2\sqrt{Ra_i} - b_i Ra_i)}{(\tau^2 {b_i}^2 - Ra_i)Ra_i}e^{\beta_i Z_i} - C_{2,i}\frac{\beta_i(\tau {b_i}^2\sqrt{Ra_i} - b_i Ra_i)}{(\tau^2 {b_i}^2 - Ra_i)Ra_i}e^{-\beta_i Z_i}\\
&\quad + C_{3,i}\frac{\gamma_{i,Im}(\tau {b_i}^2\sqrt{Ra_i} + b_i Ra_i)}{(\tau^2 {b_i}^2 - Ra_i)Ra_i}\sin(\gamma_{i,Im}Z_i)\\
&\quad - C_{4,i}\frac{\gamma_{i,Im}(\tau {b_i}^2\sqrt{Ra_i} + b_i Ra_i)}{(\tau^2 {b_i}^2 - Ra_i)Ra_i}\cos(\gamma_{i,Im}Z_i),
\end{aligned}
\tag{4.11}
$$

if γ_i is a complex number. Here, $C_{1,i}$, $C_{2,i}$, $C_{3,i}$ and $C_{4,i}$ are constants.

4.3 The Critical Rayleigh Number

By inserting the boundary conditions (3.31), (3.33), (3.34), (3.36), (3.37) and (4.3) - (4.5) into our equations (4.6)-(4.9), we obtain four homogeneous linear systems, one for each possible combination of γ_1 and γ_2. See Appendix B for the different possibilities. Each system contains ten equations and ten unknowns. For chosen values of the parameters appearing in the equations, an evaluation of γ_i will decide which system is valid for investigating real solutions.

Each system of homogeneous linear equations is represented by a 10x10 matrix. Since the four possible matrices are quite large, we have collected them in Appendix B, where they are denoted A, B, C and D. The trivial solution of the valid system is given when all the constants A_n, B_n, $C_{1,1}$, $C_{2,1}$, $C_{3,1}$, $C_{4,1}$, $C_{1,2}$, $C_{2,2}$, $C_{3,2}$ and $C_{4,2}$ are equal to zero. We want to obtain the non-trivial solution, and therefore demand the determinant of the matrix to be zero. By using the following relationship between the Rayleigh numbers in the two layers,

$$Ra_2 = \frac{K_2 {b_2}^2 {k_1}^2}{K_1 {b_1}^2 {k_2}^2} Ra_1,$$

solving for the determinant will become an eigenvalue problem for Ra_1. Notice that K_1, K_2, k_1 and k_2 have dimension, but the fraction is dimensionless.

The parameters appearing in our system are R_I, R_O, K_1, K_2, k_1, k_2, b_1, b_2, n and τ. These represent a wide variety of possible configurations and values. Several solutions for Ra_1 can be found for each fixed set of parameters. Since we are studying the onset of convection, we seek the smallest number. This value will be the critical Rayleigh number for our system. Our main interest is to examine the effect of a permeability contrast between the two layers, and to limit the area of search we fix all parameters except the permeabilities, heights and the wavenumber. For each chosen value of K_1, K_2, b_1 and b_2 we search for the wavenumber τ that minimizes Ra_1 and thereby represents the critical Rayleigh number in layer 1, $Ra_{c,1}$. Hence we can find the critical Rayleigh number $Ra_{c,1}$ as a function of the permeability contrast. A similar approach can be found in McKibbin and O'Sullivan's paper [11] for a two-layer box geometry.

Chapter 5

Results and Discussion

This chapter is devoted to a presentation and discussion of the results attained from the theoretical framework and methods described in the previous chapters. As mentioned in Chapter 4, we are interested in how the permeability contrast between the layers affects the critical Rayleigh number. By setting $K_1 = 1$, the value of K_2 will represent the permeability ratio $\frac{K_2}{K_1}$ and hence the permeability contrast. We focus on finding the critical Rayleigh number for onset of convection in the bottom layer when the permeability ratio, wavenumber and the heights are varying. To easier compare our result with previous papers, our parameters are chosen according to their values. In the following analysis we have therefore restricted the permeability K_2 to take values between 10^{-3} and 10^3 and the values of τ vary from 0.1 to 20. We will use two different height ratios of the layers, and specify these values in the analysis where they are used. The rest of the parameters are fixed, and are as follows:

$$\begin{aligned} R_I &= 1 & k_1 &= 1 \\ R_O &= 2 & k_2 &= 1 \\ K_1 &= 1 & n &= 0 \end{aligned}$$

Based on previous work by McKibbin and O'Sullivan [11] and Bringedal *et al.* [5], we expected that a variation of the integer n appearing in our solution equations (4.6)-(4.9) would have an effect on the critical Rayleigh number. We changed this variable from $n = 0$ to $n = 10$ and experienced that the critical Rayleigh number remained unchanged, although the value of the determinant changed when away from the zero point. The fact that n only appears in the radial- and azimuthal direction in our equations, while it is

also included in the vertical direction in McKibbin and O'Sullivan's solution [11], might explain why their method gave a different outcome than our approach. Hence, changing the integer n will be unnecessary in our calculations as it does not affect the critical Rayleigh number, and we have set this value to zero. As a consequence we cannot use this number to determine the preferred convective mode at onset of convection with the current procedure, and we focus only on finding critical Rayleigh numbers in the following.

We will start by evaluating the case where a variation in the wavenumber, τ, leads to a variation in the Rayleigh number in layer 1, Ra_1, for fixed permeabilities and heights. Following the outcome of this discussion we interpret the relationship between the permeability contrast and the critical Rayleigh number in layer one based on plots from our collected data.

5.1 The Effect of Varying the Wavenumber on the Rayleigh Number

By fixing the permeability contrast and heights of the layers, and making use of the values stated above, we can evaluate the Rayleigh number in layer 1 for different values of the wavenumber. We present here the case with $K_2 = 10^{-1.5}$, $b_1 = 0.3$ and $b_2 = 0.7$. The function describing the relationship between Ra_1 and τ is shown in Figure 5.1 (a). A similar analysis has been made by Masuoka *et al.* [10], which is shown in Figure 5.1 (b) for comparison. Masuoka *et al.* [10] have considered a horizontal porous medium formed by two layers, where R is the Rayleigh number in layer 2, δ is the permeability ratio $\frac{K_1}{K_2}$, h is the dimensionless height of layer 1 and a represents the wavenumber. Even though they evaluate changes in layer 2, while we investigate layer 1, the ratios of permeabilities and heights with respect to the layer of consideration are the same, hence a comparison is valid. The difference in the values of the Rayleigh number appearing on the y-axis is due to the fact that Masuoka *et al.* [10] use a different formula for this number than considered in our analysis and they have based their plot on a slightly different permeability ratio than we have used. As the purpose of the comparison is to search for similarities in the behavior of the Rayleigh number as a function of the wavenumber, the comparison is still useful for our intentions.

It can be seen from Figure 5.1(a) that there exists a clear minimum value of Ra_1 at a certain wavenumber. Similar behavior is observed by Masuoka

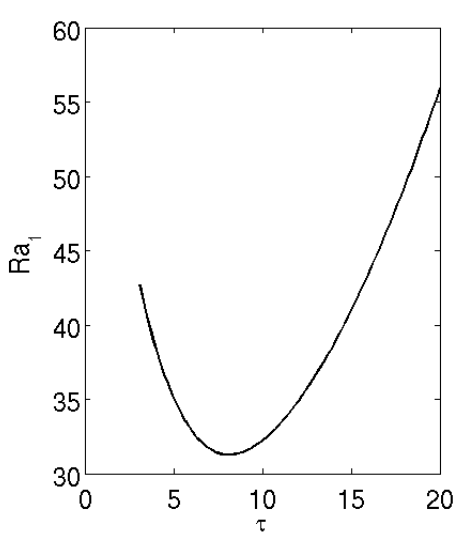

(a) Our plot of Ra_1 as a function of τ when $b_1 = 0.3$, $b_2 = 0.7$ and $\frac{K_2}{K_1} = 10^{-1.5}$.

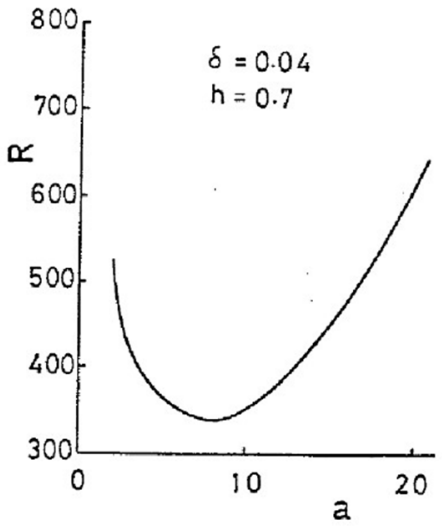

(b) A similar plot made by Masuoka *et al.* [10], where $h = 0.7$ and $\frac{K_1}{K_2} = 0.04$. This figure is a copy of Figure 4(a) in [10].

Figure 5.1: Plots of the Rayleigh number as a function of the wavenumber.

et al. [10] in their findings in Figure 5.1(b). Even though our result is presented for only one permeability ratio, we have produced graphs for a wide range of such ratios, which all imply that a minimum exist. From these findings we assume that with the fixed parameters stated above, for each value of K_1 and K_2 it is possible to find a wavenumber that minimizes the Rayleigh number in the layer of interest. This value will be the critical Rayleigh number for onset of convection, and depends on the permeability contrast between the layers.

By changing the heights of the layers to $b_1 = 0.2$ and $b_2 = 0.8$, keeping the permeabilities and the rest of the parameters the same, we found an appearance of two local minima of the wavenumber, see Figure 5.2(a). The critical Rayleigh number is determined by the lowest of these values. Masuoka *et al.* [10] also examined these heights, keeping the other parameters the same as before. Their result can be seen in Figure 5.2(b). A comparison of the graphs in Figure 5.2 shows that our results are in agreement. Masuoka *et al.* [10] investigated more height ratios in between those presented in Figure 5.1 and Figure 5.2. They found that by continuing to change the ratio of the layer

heights, a reversal of the position of the minima's would take place. Hence, they found that one specific height ratio gave two minima points of equal Rayleigh number, and consequently the critical wavenumber was discontinuous. Notice that the critical Rayleigh number was still uniquely defined. For a presentation of the graphs showing this change of position, we refer to their paper [10]. Even though we studied two height ratios, it is plausible to assume that a similar result would apply to our system if we investigated more height ratios. Our results have a limitation due to our chosen interval of τ. The observed tendency in both studies of an increasing Rayleigh number for wavenumbers larger than 20 does not exclude the possibility of a reversed tendency at larger values, and hence the possibility of more such minimum points.

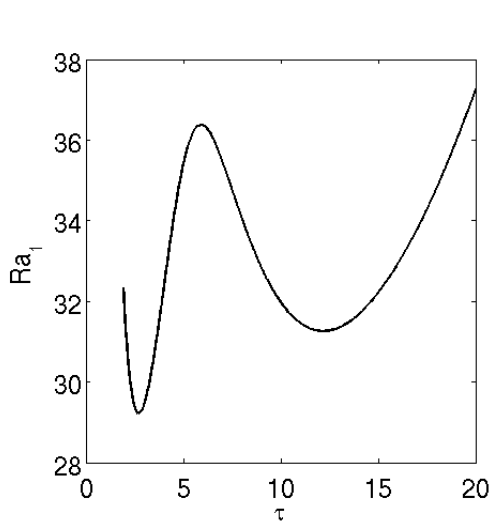

(a) Our plot of Ra_1 as a function of τ when $b_1 = 0.2$, $b_2 = 0.8$ and $\frac{K_2}{K_1} = 10^{-1.5}$.

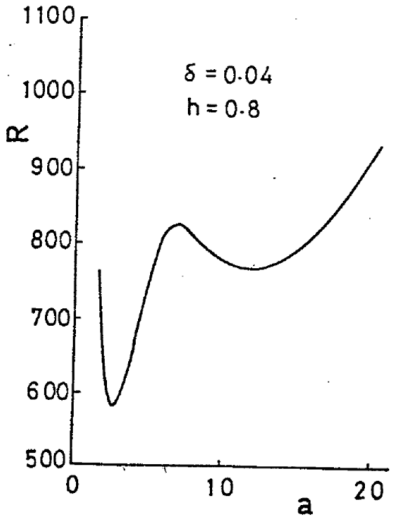

(b) A similar plot made by Masuoka *et al.* [10], where $h = 0.8$ and $\frac{K_1}{K_2} = 0.04$. This figure is a copy of Figure 4(d) in [10].

Figure 5.2: Plots of the Rayleigh number as a function of the wavenumber for new heights of the layers.

5.2 The Role of the Layer Permeabilities

As described in Section 5.1, for each permeability ratio there exist a wavenumber τ which gives the critical Rayleigh number for our chosen parameters. The plot of the critical Rayleigh number in layer 1 as a function of the permeability contrast between layer 1 and layer 2 can be seen in Figure 5.3(a). This plot is based on the heights $b_1 = 0.3$ and $b_2 = 0.7$. As mentioned in the introduction for Chapter 4, a similar analysis have been made by McKibbin and O'Sullivan [11], who considered a box shaped domain. Figure 5.3(b) displays their version of the same plot, where the nondimensional heights are equal to ours. They have ten graphs representing the different values of n, whereas we only have one graph due to the irrelevance of this integer to our solution. Their critical Rayleigh number R is based on the thickness and temperature drop of the entire system, and the conductivity and permeability of layer 1. A comparison of their result with our values for $Ra_{c,1}$ is done by applying the relation between R and $Ra_{c,1}$, given as

$$R = \frac{\delta}{\delta_1 b_1 4\pi^2} Ra_{c,1}, \tag{5.1}$$

where $\delta = \delta_1 + \delta_2$, $\delta_i = b_i \frac{h}{k_i}$ and h, k_i have dimension. By using this relation we find that our results are in good correspondence.

From Figure 5.3(a) we can see that the critical Rayleigh number in layer 1 decreases monotonically as the permeability of the upper layer is increasing. McKibbin and O'Sullivan [11] detected the same behavior. This is because a larger permeability in the top layer enhances the ability for the fluid from the bottom layer to move across the interface and into the layer above, and thereby improves the fluid flow across the border. As the permeability in the top layer continues to increase, causing a larger permeability contrast, $Ra_{c,1}$ decreases towards a very small number. When Ra_1 is slightly larger than the critical value in layer 1, and $K_2 > K_1$, the convection is expected to occur in both layers as the larger permeability in layer 2 enhances the flow conditions. Conversely, if $K_2 < K_1$, we cannot say anything about whether we have convection in layer 2 at this instant.

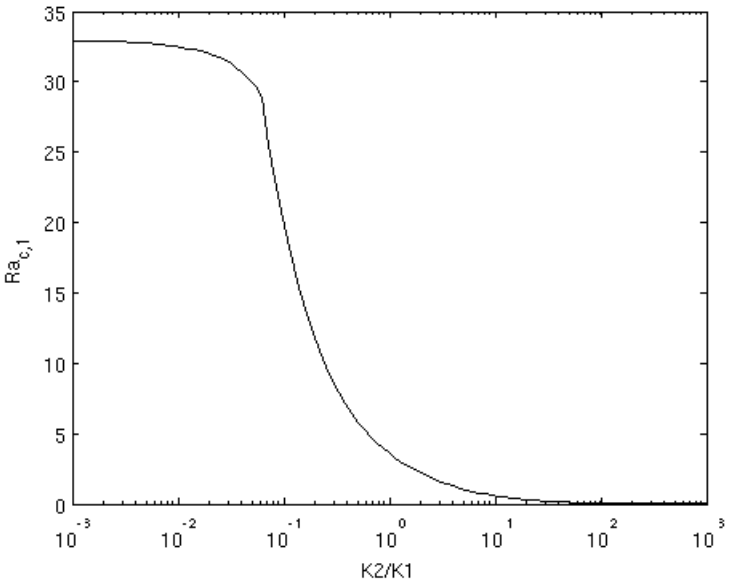

(a) Our plot of the critical Rayleigh number in layer 1 as a function of the the permeability ratio, where $b_1 = 0.3$ and $b_2 = 0.7$.

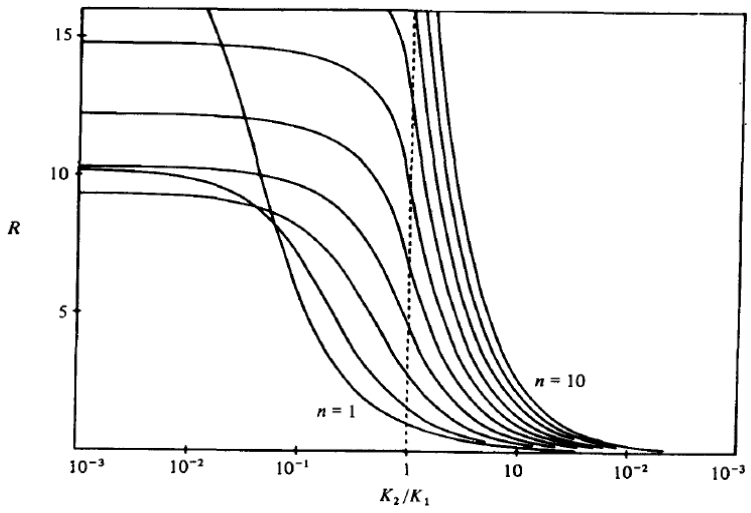

(b) Mckibbin and O'Sullivan's plot of a similar setting, where each graph corresponds to different values of n. This figure is borrowed from [11].

Figure 5.3: Corresponding plots of the Critical Rayleigh number and the permeability ratio. Note that Mckibbin and O'Sullivan [11] use R in (b), which is related to $Ra_{c,1}$ by equation (5.1).

We investigated the onset of convection for two different height ratios of the layers; $b_1 = 0.3, b_2 = 0.7$ and $b_1 = 0.2, b_2 = 0.8$. As the Rayleigh number in layer 1 is defined through the height and the temperature difference of the layer, scaling the critical Rayleigh number to account for this is made in order to simplify the comparison of the two cases. The conversion is done by using equation (3.38). A plot of the scaled critical Rayleigh number, Ra_c, as a function of the permeability contrast can be seen in Figure 5.4. The solid line is based on the heights $b_1 = 0.3$ and $b_2 = 0.7$, and the dashed line corresponds to $b_1 = 0.2$ and $b_2 = 0.8$. The tendency of a decreasing critical Rayleigh number for increasing permeability in layer two is also clear from this figure. When $K_2 < K_1$, we find that the dashed line is above the solid line, always corresponding to a larger critical Rayleigh number. It appears like a lower permeability in the top layer has an inhibiting effect on the onset of convection in the bottom layer, hence the effect is stronger for a larger height of layer 2. Conversely, when $K_2 > K_1$, the dashed line is below the solid line, always corresponding to a lower critical value, even though this is not easy to see in the graph. A larger permeability in layer 2 will enhance onset of convection, as mentioned in the above section. Naturally, when the height of this layer is larger, the positive effect is bigger and results in a lower critical Rayleigh number. When the permeabilities in the layers are equal, $K_1 = K_2$, the curves cross each other. This was expected, as both analysis then governs one homogeneous layer.

An analysis of natural convection in a homogeneous layer is done by Bringedal *et al.* in [5], where they studied onset of convection in cylindrical cordinates. Since our system will behave as one homogeneous layer when the permeabilities in both layers are equal, we expect our analyses to give identical results for the same values of R_I and R_O. Using their definition of the Rayleigh number, Ra, and our definition of Ra_1 and Ra_2, we can find a relation which can be used to convert our Rayleigh numbers in both layers into their Rayleigh number. The relation is given by

$$\frac{Ra_i}{Ra} = b_i \frac{\Delta T_i}{\Delta T}.$$

Here, ΔT_i is the temperature drop in layer i in our domain and ΔT is the temperature drop from top to bottom in Bringedal *et al.*'s annular cylinder [5]. Note that the two temperature differences are dimensional temperatures. When the permeability in both layers are equal, we use the relation stated above, and find that the converted critical Rayleigh number in both layers has the approximate value $Ra = 4\pi^2$. This result is in agreement with the analysis made by Bringedal *et al.* [5], which strengthens the validity

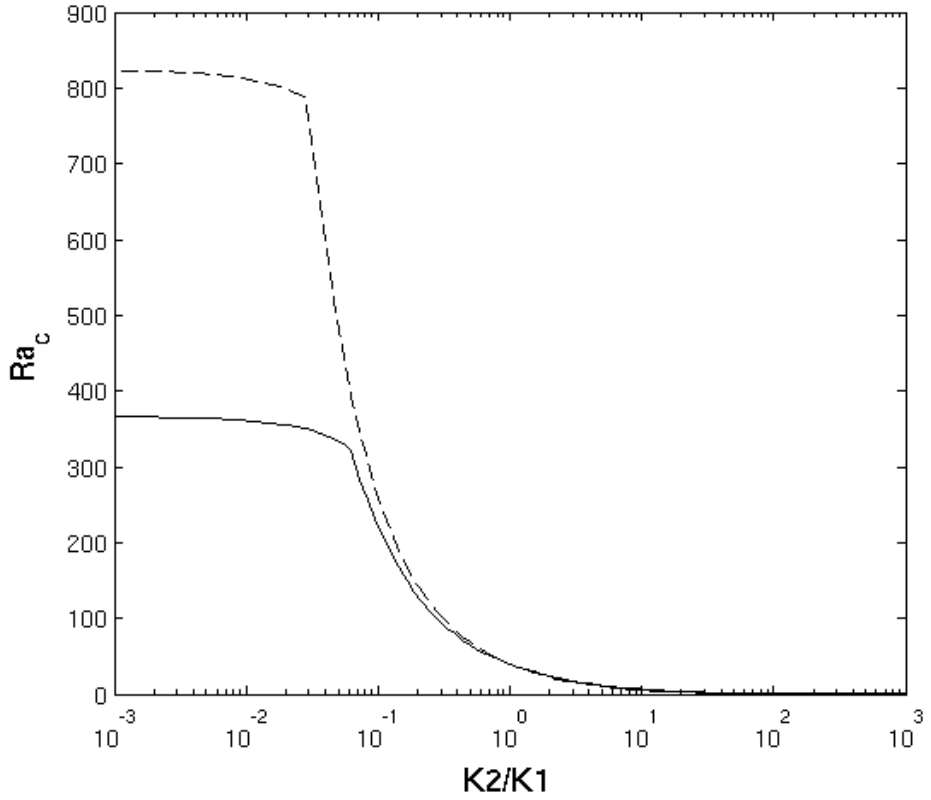

Figure 5.4: Plot of the scaled Critical Rayleigh number and the permeability contrast for two different height ratios. The solid line corresponds to $b_1 = 0.3$, $b_2 = 0.7$, and the dashed line corresponds to $b_1 = 0.2$, $b_2 = 0.8$

of our results.

Chapter 6

Conclusion

In this thesis we have studied the onset of natural convection in a two-layer porous medium located between two coaxial cylinders which are heated from below and cooled from above. A mathematical model for our system was developed, where we applied a linear stability analysis and nondimensionalized all our equations. As our model is three-dimensional, we found that solving the equations in terms of temperature and pressure was appropriate. Finally, a strategy to determine the critical Rayleigh number was established. The aim of this thesis was to investigate how permeability contrasts between the layers affect the criterion for onset of natural convection in the bottom layer.

Our analysis reveals that by fixing the permeability in layer 1, and increasing the permeability in layer 2, the growing contrast will decrease the critical Rayleigh number in the bottom layer and hence lower the criterion for onset of natural convection. This is because a larger permeability in the top layer enhances the ability of the fluid in the bottom to move across the interface and into this area. The influence is stronger for a higher upper layer. Also, by continuing to increase the permeability contrast, we find that the critical Rayleigh number in layer 1 becomes very small. When the permeability in the upper layer is larger than the permeability in the lower layer, we expect convection to occur in both areas when the Rayleigh number exceeds the critical value in layer 1. Conversely, if the permeability in the top layer is less than in the permeability in the bottom, we cannot make any conclusions about convection in layer 2.

Our findings are in agreement with previous literature on the topic. At the point where the permeability in both layers are equal, we compared our results with a previous paper involving the same geometry and boundary conditions applied to a homogeneous medium [5]. Using the same parameters

gave identical results, as expected. A comparison with similar investigations applied to a multi-layered medium in Cartesian coordinates [11] showed that the tendency of changes in the critical Rayleigh number due to an increasing permeability contrast was the same. We also found the criterion for onset of convection to be very similar. Our analysis was performed for a two-layer configuration, but the method is also suitable for a multi-layer system.

Our results are relevant in modelling of a geothermal field, as they indicate whether natural convection is present in the subsurface. The model is also applicable in benchmarking of a numerical simulator, where the results can be used to check if a numerical code is correct concerning the presence of convection.

Appendix A

Separation of Variables

We have the following pair of coupled equations:

$$\nabla_{b,i}{}^2 P_i = \frac{Ra_i}{{b_i}^3}\frac{\partial T_i}{\partial Z_i}, \tag{A-1}$$

$$\frac{1}{b_i}\frac{\partial P_i}{\partial Z_i} - \frac{Ra_i}{{b_i}^2}T_i = \nabla_{b,i}{}^2 T_i. \tag{A-2}$$

We want to solve this system to get expressions for the pressures, P_i, and the temperatures, T_i. We search for solutions by using separation of variables, where we want the solutions to be written in the following form;

$$P_i(r, \theta, Z_i) = R(r)\Theta(\theta)F_i(Z_i), \tag{A-3}$$

$$T_i(r, \theta, Z_i) = R(r)\Theta(\theta)G_i(Z_i), \tag{A-4}$$

for each of the layers $i = 1, 2$.

Note that we use same R, Θ for both pressure and temperature, and do not differentiate between the layers in these terms. Our model equations have symmetry in radial and azimuthal direction. Since the boundary conditions in the radial direction are the same for both pressure and temperature, it is reasonable to assume that $R(r)$ is equal in the expressions for P_i and T_i. Periodicity in the azimuthal direction allows us to assume that $\Theta(\theta)$ is equal in both expressions.

Since we require $\Theta(\theta)$ to be 2π-periodic, we can write it as

$$\Theta(\theta) = \cos(n\theta), \tag{A-5}$$

where n is some positive integer.

By inserting equation (A-3) and (A-4) into our original equations (A-1) and (A-2), we can find an expression for $R(r)$. This insertion, followed by a division of both equations by $\cos(n\theta)$, will result in two equations containing the separated variables $R(r)$, $F_i(Z_i)$ and $G_i(Z_i)$:

$$r^2R''(r) + rR'(r) + R(r)\Big[r^2\Big(\frac{F_i''(Z_i)}{F_i(Z_i)}\frac{1}{{b_i}^2} - \frac{Ra_i}{{b_i}^3}\frac{G_i'(Z_i)}{F_i(Z_i)}\Big) - n^2\Big] = 0, \quad \text{(A-6)}$$

$$r^2R''(r)+rR'(r)+R(r)\Big[r^2\Big(\frac{G_i''(Z_i)}{G_i(Z_i)}\frac{1}{{b_i}^2}+\frac{Ra_i}{{b_i}^2}-\frac{F_i'(Z_i)}{G_i(Z_i)}\frac{1}{b_i}\Big)-n^2\Big] = 0. \quad \text{(A-7)}$$

These equations are modified versions of Bessel's differential equation,

$$x^2\frac{d^2y}{dx^2} + x\frac{dy}{dx} + (x^2 - \alpha^2)y = 0.$$

Bessel's differential equation has solution given by Bessel functions. Our equations (A-6) and (A-7) therefore have the solutions

$$R(r) = A_nJ_n(kr) + B_nY_n(kr),$$

and

$$R(r) = C_nJ_n(qr) + D_nY_n(qr).$$

Here, J_n and Y_n are the Bessel functions of order n of first and second kind, A_n, B_n, C_n and D_n are constants and

$$\begin{aligned} k &= \sqrt{\frac{F_i''(Z_i)}{F_i(Z_i)}\frac{1}{{b_i}^2} - \frac{Ra_i}{{b_i}^3}\frac{G_i'(Z_i)}{F_i(Z_i)}}, \\ q &= \sqrt{\frac{G_i''(Z_i)}{G_i(Z_i)}\frac{1}{{b_i}^2} + \frac{Ra_i}{{b_i}^2} - \frac{F_i'(Z_i)}{G_i(Z_i)}\frac{1}{b_i}}. \end{aligned} \quad \text{(A-8)}$$

Owing to the equality of $R(r)$ in the expressions for T_i and P_i, we have that $A_n = C_n$, $B_n = D_n$ and $k = q$. By letting $k^2 = q^2 = \tau^2$ and using the presented equalities, we have our final equation for $R(r)$ given as

$$R(r) = A_n J_n(\tau r) + B_n Y_n(\tau r). \tag{A-9}$$

To find expressions for $F_i(Z_i)$ and $G_i(Z_i)$, we use (A-8) with $k = q = \tau$. Then

$$\frac{F_i''(Z_i)}{F_i(Z_i)} \frac{1}{{b_i}^2} - \frac{Ra_i}{{b_i}^3} \frac{G_i'(Z_i)}{F_i(Z_i)} = \tau^2,$$

and

$$\frac{G_i''(Z_i)}{G_i(Z_i)} \frac{1}{{b_i}^2} + \frac{Ra_i}{{b_i}^2} - \frac{F_i'(Z_i)}{G_i(Z_i)} \frac{1}{b_i} = \tau^2.$$

By introducing new variables, $F' = H$ and $G' = I$, we can convert this second-order system of two ordinary differential equations into a system of four first order ODE's. This system can be rewritten as matrix equations in the form $Ax = x'$, where x is a vector composed of our four unknown functions. Rewriting this way gives

$$\begin{bmatrix} 0 & 0 & 1 & 0 \\ 0 & 0 & 0 & 1 \\ \tau^2 {b_i}^2 & 0 & 0 & \frac{Ra_i}{b_i} \\ 0 & \tau^2 {b_i}^2 - Ra_i & b_i & 0 \end{bmatrix} \times \begin{bmatrix} F \\ G \\ H \\ I \end{bmatrix} = \begin{bmatrix} F' \\ G' \\ H' \\ I' \end{bmatrix}. \tag{A-10}$$

The eigenvalues and corresponding eigenvectors of system (A-10) give the solution. Our expressions of $F_i(Z_i)$ and $G_i(Z_i)$ are thereby composed of the four eigenvalues and the first and second components of each the corresponding eigenvectors, respectively.

The eigenvalues reads

$$\beta_i = \pm \sqrt{\tau^2 {b_i}^2 + \tau b_i \sqrt{Ra_i}}$$

and

$$\gamma_i = \pm \sqrt{\tau^2 {b_i}^2 - \tau b_i \sqrt{Ra_i}}.$$

For all possible values of the parameters, the eigenvalues β_i and the corresponding eigenvectors give real valued numbers. The eigenvalues γ_i and the associated eigenvectors might give a complex solution for some chosen parameters. Since we are only interested in real numbers we can find a real-valued solution by using the real and imaginary parts of the complex solution.

In the cases where γ_i is complex, the real part $Re(\gamma_i)$ is equal to zero and the imaginary part is

$$\gamma_{i,Im} = \pm\sqrt{\tau b_i \sqrt{Ra_i} - \tau^2 {b_i}^2},$$

where its corresponding eigenvector is real. Here the index Im is used to show that this is the imaginary part of the eigenvalue that gives a complex solution. We now denote the eigenvalues by the positive square root, and change the signs at places in our formulas where the negative values are included.

Since our final solution depends on whether γ_1 and γ_2 are complex numbers, we have four possible configurations where each gives a different solution. One possibility is that both γ_1 and γ_2 are real valued, another outcome gives both as complex numbers and the final two configurations are when one of them is a complex number and the other a real number.

Following the discussion above, our final expressions for $F_i(Z_i)$ and $G_i(Z_i)$ become:

If γ_i is real;

$$\begin{aligned}
F_i(Z_i) &= C_{1,i}e^{\beta_i Z_i} + C_{2,i}e^{-\beta_i Z_i} + C_{3,i}e^{\gamma_i Z_i} + C_{4,i}e^{-\gamma_i Z_i}, \\
G_i(Z_i) &= C_{1,i}\frac{\beta_i(\tau {b_i}^2\sqrt{Ra_i} - b_i Ra_i)}{(\tau^2 {b_i}^2 - Ra_i)Ra_i}e^{\beta_i Z_i} - C_{2,i}\frac{\beta_i(\tau {b_i}^2\sqrt{Ra_i} - b_i Ra_i)}{(\tau^2 {b_i}^2 - Ra_i)Ra_i}e^{-\beta_i Z_i} \\
&\quad - C_{3,i}\frac{\gamma_i(\tau {b_i}^2\sqrt{Ra_i} + b_i Ra_i)}{(\tau^2 {b_i}^2 - Ra_i)Ra_i}e^{\gamma_i Z_i} + C_{4,i}\frac{\gamma_i(\tau {b_i}^2\sqrt{Ra_i} + b_i Ra_i)}{(\tau^2 {b_i}^2 - Ra_i)Ra_i}e^{-\gamma_i Z_i}.
\end{aligned} \tag{A-11}$$

If γ_i is complex;

$$\begin{aligned}
F_i(Z_i) &= C_{1,i}e^{\beta_i Z_i} + C_{2,i}e^{-\beta_i Z_i} + C_{3,i}\cos(\gamma_{i,Im}Z_i) + C_{4,i}\sin(\gamma_{i,Im}Z_i),\\
G_i(Z_i) &= C_{1,i}\frac{\beta_i(\tau {b_i}^2\sqrt{Ra_i} - b_i Ra_i)}{(\tau^2 {b_i}^2 - Ra_i)Ra_i}e^{\beta_i Z_i} - C_{2,i}\frac{\beta_i(\tau {b_i}^2\sqrt{Ra_i} - b_i Ra_i)}{(\tau^2 {b_i}^2 - Ra_i)Ra_i}e^{-\beta_i Z_i}\\
&\quad + C_{3,i}\frac{\gamma_{i,Im}(\tau {b_i}^2\sqrt{Ra_i} + b_i Ra_i)}{(\tau^2 {b_i}^2 - Ra_i)Ra_i}\sin(\gamma_{i,Im}Z_i)\\
&\quad - C_{4,i}\frac{\gamma_{i,Im}(\tau {b_i}^2\sqrt{Ra_i} + b_i Ra_i)}{(\tau^2 {b_i}^2 - Ra_i)Ra_i}\cos(\gamma_{i,Im}Z_i).
\end{aligned} \tag{A-12}$$

In the expressions above, $C_{1,i}$, $C_{2,i}$, $C_{3,i}$ and $C_{4,i}$ are constants.

Summing up, equation (A-5), (A-9) and (A-11)-(A-12) give us the final solutions for P and T;

$$P_1(r,\theta,Z_1) = \Big[A_n J_n(\tau r) + B_n Y_n(\tau r)\Big]\cos(n\theta)F_1(Z_1), \tag{A-13}$$

$$P_2(r,\theta,Z_2) = \Big[A_n J_n(\tau r) + B_n Y_n(\tau r)\Big]\cos(n\theta)F_2(Z_2), \tag{A-14}$$

$$T_1(r,\theta,Z_1) = \Big[A_n J_n(\tau r) + B_n Y_n(\tau r)\Big]\cos(n\theta)G_1(Z_1), \tag{A-15}$$

$$T_2(r,\theta,Z_2) = \Big[A_n J_n(\tau r) + B_n Y_n(\tau r)\Big]\cos(n\theta)G_2(Z_2), \tag{A-16}$$

where the expressions for $F_1(Z_1)$, $F_2(Z_2)$, $G_1(Z_1)$ and $G_2(Z_2)$ depend on the values of γ_1 and γ_2, as stated in equation (A-11)-(A-12).

Appendix B

The Matrices

Four homogeneous linear systems of equations are given when the boundary conditions are applied to our expressions for T and P. These systems can be represented by matrices, which we will denote A, B, C and D.

Each matrix represent one of the four possible configurations of γ_1 and γ_2:

A: The valid matrix when both γ_1, γ_2 are real.

B: The valid matrix when γ_1 is complex and γ_2 is real.

C: The valid matrix when γ_1 is real and γ_2 is complex.

D: The valid matrix when both γ_1 and γ_2 are complex.

Each row in the matrices corresponds to one of the boundary conditions (BC) in the following way:

Row 1 - BC (4.3), for layer 1
Row 2 - BC (3.31), for layer 1
Row 3 - BC (4.3), for layer 2
Row 4 - BC (3.31), for layer 2
Row 5 - BC (3.34)
Row 6 - BC (4.5)
Row 7 - BC (3.36)
Row 8 - BC (3.37)

Row 9 - BC (4.4)
Row10 - BC (3.33)

The matrices are multiplied with

$$\begin{bmatrix} A_n \\ B_n \\ C_{1,1} \\ C_{2,1} \\ C_{3,1} \\ C_{4,1} \\ C_{1,2} \\ C_{2,2} \\ C_{3,2} \\ C_{4,2} \end{bmatrix}.$$

To ease the notation within each matrix, the following abbreviations have been used:

$$\begin{aligned}
\beta_i &= \sqrt{\tau^2 {b_i}^2 + \tau b_i \sqrt{Ra_i}}, \\
\gamma_i &= \sqrt{\tau^2 {b_i}^2 - \tau b_i \sqrt{Ra_i}} \quad \text{when } \gamma_i \text{ is a real number,} \\
\gamma_{i,Im} &= \sqrt{\tau b_i \sqrt{Ra_i} - \tau^2 {b_i}^2} \quad \text{when } \gamma_i \text{ is a complex number,} \\
M_i &= \tau {b_i}^2 \sqrt{Ra_1} - b_i Ra_i, \\
N_i &= \tau {b_i}^2 \sqrt{Ra_1} + b_i Ra_i, \\
Q_i &= (\tau^2 {b_i}^2 - Ra_i) Ra_i.
\end{aligned}$$

The matrices are presented in the following pages.

$$
A=\begin{bmatrix}
0 & 0 & \beta_1 & -\beta_1 & \gamma_1 & -\gamma_1 & 0 & 0 & 0 & 0 \\
0 & 0 & \frac{\beta_1 M_1}{Q_1} & -\frac{\beta_1 M_1}{Q_1} & -\frac{\gamma_1 N_1}{Q_1} & \frac{\gamma_1 N_1}{Q_1} & 0 & 0 & 0 & 0 \\
0 & 0 & 0 & 0 & 0 & 0 & \beta_2 e^{\beta_2} & -\beta_2 e^{-\beta_2} & \gamma_2 e^{\gamma_2} & -\gamma_2 e^{-\gamma_2} \\
0 & 0 & 0 & 0 & 0 & 0 & \frac{\beta_2 M_2}{Q_2} e^{\beta_2} & -\frac{\beta_2 M_2}{Q_2} e^{-\beta_2} & -\frac{\gamma_2 N_2}{Q_2} e^{\gamma_2} & \frac{\gamma_2 N_2}{Q_2} e^{-\gamma_2} \\
0 & 0 & \frac{b_1}{k_1}\frac{\beta_1 M_1}{Q_1} e^{\beta_1} & -\frac{b_1}{k_1}\frac{\beta_1 M_1}{Q_1} e^{-\beta_1} & -\frac{b_1}{k_1}\frac{\gamma_1 N_1}{Q_1} e^{\gamma_1} & \frac{b_1}{k_1}\frac{\gamma_1 N_1}{Q_1} e^{-\gamma_1} & -\frac{b_2}{k_2}\frac{\beta_2 M_2}{Q_2} & \frac{b_2}{k_2}\frac{\beta_2 M_2}{Q_2} & \frac{b_2}{k_2}\frac{\gamma_2 N_2}{Q_2} & -\frac{b_2}{k_2}\frac{\gamma_2 N_2}{Q_2} \\
0 & 0 & k_1\beta_1 e^{\beta_1} - \frac{Ra_1 k_1}{b_1}\frac{\beta_1 M_1}{Q_1} e^{\beta_1} & -k_1\beta_1 e^{-\beta_1} + \frac{Ra_1 k_1}{b_1}\frac{\beta_1 M_1}{Q_1} e^{-\beta_1} & k_1\gamma_1 e^{\gamma_1} + \frac{Ra_1 k_1}{b_1}\frac{\gamma_1 N_1}{Q_1} e^{\gamma_1} & -k_1\gamma_1 e^{-\gamma_1} - \frac{Ra_1 k_1}{b_1}\frac{\gamma_1 N_1}{Q_1} e^{-\gamma_1} & -k_2\beta_2 + \frac{Ra_2 k_2}{b_2}\frac{\beta_2 M_2}{Q_2} & k_2\beta_2 - \frac{Ra_2 k_2}{b_2}\frac{\beta_2 M_2}{Q_2} & -k_2\gamma_2 - \frac{Ra_2 k_2}{b_2}\frac{\gamma_2 N_2}{Q_2} & k_2\gamma_2 + \frac{Ra_2 k_2}{b_2}\frac{\gamma_2 N_2}{Q_2} \\
0 & 0 & \frac{b_1 k_1}{K_1} e^{\beta_1} & \frac{b_1 k_1}{K_1} e^{-\beta_1} & \frac{b_1 k_1}{K_1} e^{\gamma 1} & \frac{b_1 k_1}{K_1} e^{-\gamma_1} & -\frac{b_2 k_2}{K_2} & -\frac{b_2 k_2}{K_2} & -\frac{b_2 k_2}{K_2} & -\frac{b_2 k_2}{K_2} \\
0 & 0 & \frac{{\beta_1}^2 M_1}{Q_1} e^{\beta_1} & \frac{{\beta_1}^2 M1}{Q1} e^{-\beta_1} & -\frac{{\gamma_1}^2 N_1}{Q_1} e^{\gamma_1} & -\frac{{\gamma_1}^2 N_1}{Q_1} e^{-\gamma_1} & -\frac{{\beta_2}^2 M_2}{Q_2} & -\frac{{\beta_2}^2 M_2}{Q_2} & \frac{{\gamma_2}^2 N_2}{Q_2} & \frac{{\gamma_2}^2 N_2}{Q_2} \\
J_n'(\tau R_I) & Y_n'(\tau R_I) & 0 & 0 & 0 & 0 & 0 & 0 & 0 & 0 \\
J_n'(\tau R_0) & Y_n'(\tau R_0) & 0 & 0 & 0 & 0 & 0 & 0 & 0 & 0
\end{bmatrix}
$$

$$
B=\begin{bmatrix}
0 & 0 & \beta_1 & -\beta_1 & 0 & -\gamma_1 & 0 & 0 & 0 & 0 \\
0 & 0 & \frac{\beta_1 M_1}{Q_1} & -\frac{\beta_1 M_1}{Q_1} & 0 & -\frac{\gamma_1 N_1}{Q_1} & 0 & 0 & 0 & 0 \\
0 & 0 & 0 & 0 & 0 & 0 & \beta_2 e^{\beta_2} & -\beta_2 e^{-\beta_2} & \gamma_2 e^{\gamma_2} & -\gamma_2 e^{-\gamma_2} \\
0 & 0 & 0 & 0 & 0 & 0 & \frac{\beta_2 M_2}{Q_2} e^{\beta_2} & -\frac{\beta_2 M_2}{Q_2} e^{-\beta_2} & -\frac{\gamma_2 N_2}{Q_2} e^{\gamma_2} & \frac{\gamma_2 N_2}{Q_2} e^{-\gamma_2} \\
0 & 0 & \frac{b_1}{k_1}\frac{\beta_1 M_1}{Q_1} e^{\beta_1} & -\frac{b_1}{k_1}\frac{\beta_1 M_1}{Q_1} e^{-\beta_1} & \frac{b_1}{k_1}\frac{\gamma_{1,Im} N_1}{Q_1}\sin(\gamma_{1,Im}) & -\frac{b_1}{k_1}\frac{\gamma_{1,Im} N_1}{Q_1}\cos(\gamma_{1,Im}) & -\frac{b_1}{k_1}\frac{\beta_2 M_2}{Q_2} & \frac{b_2}{k_2}\frac{\beta_2 M_2}{Q_2} & \frac{b_2}{k_2}\frac{\gamma_2 N_2}{Q_2} & -\frac{b_2}{k_2}\frac{\gamma_2 N_2}{Q_2} \\
0 & 0 & k_1\beta_1 e^{\beta_1} - \frac{Ra_1 k_1}{b_1}\frac{\beta_1 M_1}{Q_1} e^{\beta_1} & -k_1\beta_1 e^{-\beta_1} + \frac{Ra_1 k_1}{b_1}\frac{\beta_1 M_1}{Q_1} e^{-\beta_1} & -k_1\gamma_{1,Im}\sin(\gamma_{1,Im}) - \frac{Ra_1 k_1}{b_1}\frac{\gamma_{1,Im} N_1}{Q_1}\sin(\gamma_{1,Im}) & k_1\gamma_{1,Im}\cos(\gamma_{1,Im}) + \frac{Ra_1 k_1}{b_1}\frac{\gamma_{1,Im} N_1}{Q_1}\cos(\gamma_{1,Im}) & -k_2\beta_2 + \frac{Ra_2 k_2}{b_2}\frac{\beta_2 M_2}{Q_2} & k_2\beta_2 - \frac{Ra_2 k_2}{b_2}\frac{\beta_2 M_2}{Q_2} & -k_2\gamma_2 - \frac{Ra_2 k_2}{b_2}\frac{\gamma_2 N_2}{Q_2} & k_2\gamma_2 + \frac{Ra_2 k_2}{b_2}\frac{\gamma_2 N_2}{Q_2} \\
0 & 0 & \frac{b_1 k_1}{K_1} e^{\beta_1} & \frac{b_1 k_1}{K_1} e^{-\beta_1} & \frac{b_1 k_1}{K_1}\cos(\gamma_{1,Im}) & \frac{b_1 k_1}{K_1}\sin(-\gamma_{1,Im}) & -\frac{b_2 k_2}{K_2} & -\frac{b_2 k_2}{K_2} & -\frac{b_2 k_2}{K_2} & -\frac{b_2 k_2}{K_2} \\
0 & 0 & \frac{{\beta_1}^2 M_1}{Q_1} e^{\beta_1} & \frac{{\beta_1}^2 M1}{Q1} e^{-\beta_1} & \frac{{\gamma_{1,Im}}^2 N_1}{Q_1}\cos(\gamma_{1,Im}) & \frac{{\gamma_{1,Im}}^2 N_1}{Q_1}\sin(\gamma_{1,Im}) & -\frac{{\beta_2}^2 M_2}{Q_2} & -\frac{{\beta_2}^2 M_2}{Q_2} & \frac{{\gamma_2}^2 N_2}{Q_2} & \frac{{\gamma_2}^2 N_2}{Q_2} \\
J_n'(\tau R_I) & Y_n'(\tau R_I) & 0 & 0 & 0 & 0 & 0 & 0 & 0 & 0 \\
J_n'(\tau R_0) & Y_n'(\tau R_0) & 0 & 0 & 0 & 0 & 0 & 0 & 0 & 0
\end{bmatrix}
$$

$$
C=\begin{bmatrix}
0 & 0 & \beta_1 & -\beta_1 & \gamma_1 & -\gamma_1 & 0 & 0 & 0 & 0 \\
0 & 0 & \frac{\beta_1 M_1}{Q_1} & -\frac{\beta_1 M_1}{Q_1} & -\frac{\gamma_1 N_1}{Q_1} & \frac{\gamma_1 N_1}{Q_1} & 0 & 0 & 0 & 0 \\
0 & 0 & 0 & 0 & 0 & 0 & \beta_2 e^{\beta_2} & -\beta_2 e^{-\beta_2} & -\gamma_{2,Im}\sin(\gamma_{2,Im}) & \gamma_{2,Im}\cos(\gamma_{2,Im}) \\
0 & 0 & 0 & 0 & 0 & 0 & \frac{\beta_2 M_2}{Q_2} e^{\beta_2} & -\frac{\beta_2 M_2}{Q_2} e^{-\beta_2} & \frac{\gamma_{2,Im} N_2}{Q_2}\sin(\gamma_{2,Im}) & -\frac{\gamma_{2,Im} N_2}{Q_2}\cos(\gamma_{2,Im}) \\
0 & 0 & \frac{b_1}{k_1}\frac{\beta_1 M_1}{Q_1} e^{\beta_1} & -\frac{b_1}{k_1}\frac{\beta_1 M_1}{Q_1} e^{-\beta_1} & -\frac{b_1}{k_1}\frac{\gamma_1 N_1}{Q_1} e^{\gamma_1} & \frac{b_1}{k_1}\frac{\gamma_1 N_1}{Q_1} e^{-\gamma_1} & -\frac{b_2}{k_2}\frac{\beta_2 M_2}{Q_2} & \frac{b_2}{k_2}\frac{\beta_2 M_2}{Q_2} & 0 & \frac{b_2}{k_2}\frac{\gamma_{2,Im} N_2}{Q_2} \\
0 & 0 & k_1\beta_1 e^{\beta_1} - \frac{Ra_1 k_1}{b_1}\frac{\beta_1 M_1}{Q_1} e^{\beta_1} & -k_1\beta_1 e^{-\beta_1} + \frac{Ra_1 k_1}{b_1}\frac{\beta_1 M_1}{Q_1} e^{-\beta_1} & k_1\gamma_1 e^{\gamma_1} + \frac{Ra_1 k_1}{b_1}\frac{\gamma_1 N_1}{Q_1} e^{\gamma_1} & -k_1\gamma_1 e^{-\gamma_1} - \frac{Ra_1 k_1}{b_1}\frac{\gamma_1 N_1}{Q_1} e^{-\gamma_1} & -k_2\beta_2 + \frac{Ra_2 k_2}{b_2}\frac{\beta_2 M_2}{Q_2} & k_2\beta_2 - \frac{Ra_2 k_2}{b_2}\frac{\beta_2 M_2}{Q_2} & 0 & -k_2\gamma_{2,Im} - \frac{Ra_2 k_2}{b_2}\frac{\gamma_{2,Im} N_2}{Q_2} \\
0 & 0 & \frac{b_1 k_1}{K_1} e^{\beta_1} & \frac{b_1 k_1}{K_1} e^{-\beta_1} & \frac{b_1 k_1}{K_1} e^{\gamma_1} & \frac{b_1 k_1}{K_1} e^{-\gamma_1} & -\frac{b_2 k_2}{K_2} & -\frac{b_2 k_2}{K_2} & -\frac{b_2 k_2}{K_2} & 0 \\
0 & 0 & \frac{{\beta_1}^2 M_1}{Q_1} e^{\beta_1} & \frac{{\beta_1}^2 M1}{Q1} e^{-\beta_1} & -\frac{{\gamma_1}^2 N_1}{Q_1} e^{\gamma_1} & -\frac{{\gamma_1}^2 N_1}{Q_1} e^{-\gamma_1} & -\frac{{\beta_2}^2 M_2}{Q_2} & -\frac{{\beta_2}^2 M_2}{Q_2} & -\frac{{\gamma_{2,Im}}^2 N_2}{Q_2} & 0 \\
J_n'(\tau R_I) & Y_n'(\tau R_I) & 0 & 0 & 0 & 0 & 0 & 0 & 0 & 0 \\
J_n'(\tau R_0) & Y_n'(\tau R_0) & 0 & 0 & 0 & 0 & 0 & 0 & 0 & 0
\end{bmatrix}
$$

(55)

$$
D=\begin{bmatrix}
0 & 0 & \beta_1 & -\beta_1 & 0 & \gamma_{1,Im} & 0 & 0 & 0 & 0 \\
0 & 0 & \frac{\beta_1 M_1}{Q_1} & -\frac{\beta_1 M_1}{Q_1} & 0 & -\frac{\gamma_{1,Im} N_1}{Q_1} & 0 & 0 & 0 & 0 \\
0 & 0 & 0 & 0 & 0 & 0 & \beta_2 e^{\beta_2} & -\beta_2 e^{-\beta_2} & -\gamma_2 \sin(\gamma_{2,Im}) & \gamma_{2,Im}\cos(\gamma_{2,Im}) \\
0 & 0 & 0 & 0 & 0 & 0 & \frac{\beta_2 M_2}{Q_2} e^{\beta_2} & -\frac{\beta_2 M_2}{Q_2} e^{-\beta_2} & \frac{\gamma_{2,Im} N_2}{Q_2}\sin(\gamma_{2,Im}) & -\frac{\gamma_{2,Im} N_2}{Q_2}\cos(\gamma_{2,Im}) \\
0 & 0 & \frac{b_1}{k_1}\frac{\beta_1 M_1}{Q_1} e^{\beta_1} & -\frac{b_1}{k_1}\frac{\beta_1 M_1}{Q_1} e^{-\beta_1} & \frac{b_1}{k_1}\frac{\gamma_{1,Im} N_1}{Q_1}\sin(\gamma_{1,Im}) & -\frac{b_1}{k_1}\frac{\gamma_{1,Im} N_1}{Q_1}\cos(\gamma_{1,Im}) & -\frac{b_2}{k_2}\frac{\beta_2 M_2}{Q_2} & \frac{b_2}{k_2}\frac{\beta_2 M_2}{Q_2} & 0 & \frac{b_2}{k_2}\frac{\gamma_{2,Im} N_2}{Q_2} \\
0 & 0 & k_1\beta_1 e^{\beta_1} - \frac{Ra_1 k_1}{b_1}\frac{\beta_1 M_1}{Q_1} e^{\beta_1} & -k_1\beta_1 e^{-\beta_1} + \frac{Ra_1 k_1}{b_1}\frac{\beta_1 M_1}{Q_1} e^{-\beta_1} & -k_1\gamma_{1,Im}\sin(\gamma_{1,Im}) - \frac{Ra_1 k_1}{b_1}\frac{\gamma_{1,Im} N_1}{Q_1}\sin(\gamma_{1,Im}) & k_1\gamma_{1,Im}\cos(\gamma_{1,Im}) + \frac{Ra_1 k_1}{b_1}\frac{\gamma_{1,Im} N_1}{Q_1}\cos(\gamma_{1,Im}) & -k_2\beta_2 + \frac{Ra_2 k_2}{b_2}\frac{\beta_2 M_2}{Q_2} & k_2\beta_2 - \frac{Ra_2 k_2}{b_2}\frac{\beta_2 M_2}{Q_2} & 0 & -k_2\gamma_{2,Im} - \frac{Ra_2 k_2}{b_2}\frac{\gamma_{2,Im} N_2}{Q_2} \\
0 & 0 & \frac{b_1 k_1}{K_1} e^{\beta_1} & \frac{b_1 k_1}{K_1} e^{-\beta_1} & \frac{b_1 k_1}{K_1}\cos(\gamma_{1,Im}) & \frac{b_1 k_1}{K_1}\sin(\gamma_{1,Im}) & -\frac{b_2 k_2}{K_2} & -\frac{b_2 k_2}{K_2} & -\frac{b_2 k_2}{K_2} & 0 \\
0 & 0 & \frac{{\beta_1}^2 M_1}{Q_1} e^{\beta_1} & \frac{{\beta_1}^2 M1}{Q1} e^{-\beta_1} & \frac{{\gamma_{1,Im}}^2 N_1}{Q_1}\cos(\gamma_{1,Im}) & \frac{{\gamma_{1,Im}}^2 N_1}{Q_1}\sin(\gamma_{1,Im}) & -\frac{{\beta_2}^2 M_2}{Q_2} & -\frac{{\beta_2}^2 M_2}{Q_2} & -\frac{{\gamma_{2,Im}}^2 N_2}{Q_2} & 0 \\
J_n'(\tau R_I) & Y_n'(\tau R_I) & 0 & 0 & 0 & 0 & 0 & 0 & 0 & 0 \\
J_n'(\tau R_0) & Y_n'(\tau R_0) & 0 & 0 & 0 & 0 & 0 & 0 & 0 & 0
\end{bmatrix}
$$

Bibliography

[1] H. H. Bau and K. E. Torrance. Onset of convection in a permeable medium between vertical coaxial cylinders. *Physics of Fluids*, 24(3):382–385, 1981.

[2] J. Bear. *Dynamics of fluids in porous media.* Dover Publications, 1988.

[3] A. Bejan and A. D. Kraus. *Heat transfer handbook.* John Wiley and Sons, 2003.

[4] C. Bringedal. Linear and nonlinear convection in porous media between coaxial cylinders. Master's thesis, University of Bergen, 2011.

[5] C. Bringedal, I. Berre, J. M. Nordbotten, and D. A. S. Rees. Linear and nonlinear convection in porous media between coaxial cylinders. *Physics of fluids*, 23(9), 2011.

[6] H. Gupta and S. Roy. *Geothermal Energy-An alternative resource for the 21st century.* Elsevier, 1 edition, 2007.

[7] C. W. Horton and F. T. Rogers. Convection currents in a porous medium. *Journal of Applied Physics*, 16(6):367–370, 1945.

[8] A. Kagel, D. Bates, and K. Gawell. *A guide to geothermal energy and the environment.* United States. Dept. of Energy. Geothermal Division, 2005.

[9] E. R. Lapwood. Convection of a fluid in a porous medium. *Mathematical Proceedings of the Cambridge Philosophical Society*, 44:508–521, 1948.

[10] T. Masuoka, T. Katsuhara, Y. Nakazono, and S. Isozaki. Onset of convection and flow patterns in a porous layer of two different media. *Heat Transfer Japanese Research*, 7(2):39–52, 1979.

[11] R. McKibbin and M. J. O'Sullivan. Onset of convection in a layered porous medium heated from below. *Journal of Fluid Mechanics*, 96(02):375–393, 1980.

[12] R. McKibbin and M. J. O'Sullivan. Heat transfer in a layered porous medium heated from below. *Journal of Fluid Mechanics*, 111(02):141–173, 1981.

[13] M. B. Moranville, D. P. Kessler, and R. A. Greenkorn. Dispersion in layared porous media. *AIChE Journal*, 23(06):786–794, 1977.

[14] D. A. Nield and A. Bejan. *Convection in Porous Media*. Springer, 3 edition, 2006.

[15] J. M. Nordbotten and M. A. Celia. *Geological Storage of CO_2*. Wiley, 2012.

[16] Ø. Pettersen. *Grunnkurs i RESERVOARMEKANIKK*. Matematisk institutt, Universitetet i Bergen, 1990.

[17] D. Pribnow and R. Schellschmidt. Thermal tracking of thermal upper crustal fluid flow in the Rhine Graben. *Geophysical research letters*, 27(13):1957–1960, 2000.

[18] D. A. S. Rees, A. P. Bassom, and G. Genç. Weakly nonlinear convection in a porous layer with multiple horizontal partitions. *Transport in porous media*, 103(3):437–448, 2014.

[19] D. A. S. Rees and D. S. Riley. The three-dimensionality of finite-amplitude convection in a layered porous medium heated from below. *Journal of Fluid Mechanics*, 211:437–461, 1990.

[20] J. W. Tester, B. Anderson, A. Batchelor, D. Blackwell, R. DiPippo, E. Drake, J. Garnish, B. Livesay, M. C. Moore, K. Nichols, et al. The future of geothermal energy: impact of Enhanced Geothermal Systems (EGS) on the United States in the 21st Century. *Final Report to the US Department of Energy Geothermal Technologies Program. Cambridge, MA.: Massachusetts Institute of Technology*, 2006.